

# CHALMERS



## DC High Voltage Connection Systems for Offshore Wind Turbines

Master of Science Thesis

**SERGIO GARCÍA COLINO**

Department of Energy and Environment  
*Division of Electric Power Engineering*  
CHALMERS UNIVERSITY OF TECHNOLOGY  
Göteborg, Sweden 2010



# DC High Voltage Connection Systems for Offshore Wind Turbines

Master of Science Thesis

SERGIO GARCÍA COLINO

Department of Energy and Environment  
*Division of Electric Power Engineering*  
CHALMERS UNIVERSITY OF TECHNOLOGY

Göteborg, Sweden 2010

DC High Voltage Connection Systems for Offshore Wind Turbines

Master of Science Thesis

SERGIO GARCÍA COLINO

© **SERGIO GARCÍA COLINO, 2010**

Department of Energy and Environment

Division of Electric Power Engineering

Chalmers University of Technology

SE-412 96 Göteborg

Sweden

Telephone: + 46 (0)31-772 1000

Cover:

Cape Wind Project, America's First Offshore Wind Farm on Nantucket Sound.

Reference to more extensive information [<http://www.capewind.org/>]

Chalmers Bibliotek, Reproservice

Göteborg, Sweden 2010

# Acknowledgments

This work has been carried out at the Division of Electrical Power Engineering, Department of Energy and Environment at Chalmers University of Technology, Sweden. Facilities provided by the Department during the Master Thesis work are gratefully acknowledged.

I would like to thank my supervisor and examiner Dr. Torbjörn Thiringer for his supervision, patience and for giving me the opportunity to work on such a challenging project. Also thanks to the PhD student Poopak Roshanfekr Fard for her helpful suggestions, I wish you good luck with your research.

During my work, I had the privilege to share the work place with other researchers. It was a great experience to spend this time together, with the brain storm ideas, enquiring questions, laughs, hard work and always learning. My thanks go specially to Saman Babaei, Sylvain Lechat Sanjuan, Francisco Montes, Carlos Castillo, Mehdi Joe and, of course, Pramod Bangalore who always kept an open door to all my doubts and questions. I would like to thank Uge for this summer and for his invaluable help, always there to listen me and laugh together. Also thank to the great friends that I had the opportunity to make during this incredible year, you know of whom I am talking.

This Thesis was almost the last step of a really long and tough trip that started in September of 2002 in Madrid. Then, most of us did not expected to reach the end together and become so close friends, but now I realize that without you I could not do it. For my partners of sufferings, “the five horsemen”, we’ve got it!

Also, to my true friends at school, university, neighbourhood, thanks for all the unforgettable moments that we have spent together and for the ones that will come.

Finally, at the end but not for that less important, I would like to thank my family for supporting me all the time and believe in me. My heartfelt gratitude goes to my mother, father and brother, that have been standing me all of these years in the bad and the good moments, and I know it was not easy at all. Now is my turn to make it up to you. Thanks for being the best family that I could ever have.



# DC High Voltage Connection Systems for Offshore Wind Turbines

Master of Science Thesis

SERGIO GARCÍA COLINO

Department of Energy and Environment

Division of Electric Power Engineering

Chalmers University of Technology

## **Abstract**

Renewable energies have been taking an important role in the disperse generation in the last years. Within these resources one of the most important and developed is the wind turbine technology.

This work investigates a basic and robust system that could be suitable to use in applications where wind turbines are connected to a DC link. Then, it could be possible to increase the efficiency of each wind turbine system and save costs in the transformer platform at the output of the wind farm. Here a system consisting of a 2 MW Permanent Magnet Synchronous Generator (PMSG), a diode rectifier and a boost converter is analysed.

The studies carried out in this project are based on simulations made with MATLAB Simulink. Considering an output voltage of 6.75 kV, the results shown that is possible to implement this system to increase the efficiency of each individual wind turbine and, as an advantage due to the DC link, have more control on the voltage levels and the output power that is supplied. Also, the losses through the components of the system were found to be small.

**Key words:** DC High Voltage (HVDC), Boost converter, Permanent Magnet Synchronous Generator, Full Bridge Diode Rectifier, Offshore Wind Turbines.





Contents	
ACKNOWLEDGMENTS	I
ABSTRACT	III
NOTATIONS	VII
1 CHAPTER ONE	1
1.1 Problem overview	1
1.2 Previous work	2
1.3 Purpose of the work	2
1.4 Outline of the thesis	2
2 CHAPTER TWO	4
2.1 Wind turbines	4
2.1.1 Energy conversion of wind turbines	4
2.1.2 Variable speed wind turbines	5
2.2 Wind turbine and gearbox models	5
2.3 Model of the generator	6
2.4 Offshore wind farms	7
2.5 DC connected wind turbines and high voltage systems	7
2.5.1 General view of wind parks	7
2.5.2 Offshore system configurations	8
2.5.3 High voltage DC transmission	10
3 CHAPTER THREE	11
3.1 Why synchronous generator?	11
3.2 System topology	11
3.2.1 Wind turbine	12
3.2.2 Electrically magnetized synchronous generator	12
3.2.3 Permanent magnet synchronous generator	12
3.2.4 Diode rectifier	13
3.2.5 Boost converter	15
3.2.6 Variable capacitor	18
4 CHAPTER FOUR	19
4.1 SimPowerSystems	19
4.1.1 Permanent magnet synchronous machine block	19
4.1.2 Universal Bridge block	20
4.1.3 More blocks used in the simulations	20
4.2 The system specifications	22
4.2.1 Characteristics of the wind turbine	22
4.2.2 Characteristics of the generator	23

4.3	Verification studies	24
4.3.1	Calculation of the generator output voltage values	24
4.3.2	Three-phase full bridge diode rectifier	26
4.4	Design of the boost converter	33
4.5	Simulation of the boost converter	36
5	CHAPTER FIVE	41
5.1	Design of the inductor	41
5.2	Calculation of losses	44
6	CHAPTER SIX	46
6.1	Future work	46
7	REFERENCES	47
	APPENDIX	49

# Notations

## Symbols

$A_{core}$	Core area in the inductor	[mm <sup>2</sup> ]
$A_d$	Average value of the output voltage of the rectifier	[V]
$B_{av}$	Average flux density in the inductor	[T]
$C_d$	Filter Capacitor	[F]
$C_P(\lambda, \beta)$	Aerodynamic efficiency	
$C_{out(min)}$	Minimum output capacitor	[F]
$D$	Switch duty ratio	
$D_1$	One of the dimension of the inductor	[mm]
$E_k$	Kinetic energy	[J]
$f$	Frequency	[Hz]
$f_s$	Switching frequency	[Hz]
$h$	Length of the inductor air-gap	[mm]
$I_{av}$	Average current through the inductor	[A]
$I_d$	DC side rectifier output current	[A]
$I_{d,av}$	DC average current	[A]
$i_d$	Stator current in $d$ -axis	[A]
$I_{L,lim}$	Average value of the inductor at the boundary	[A]
$i_L(t)$	Current over the inductor of the Boost converter	[A]
$i_{L,peak}$	Peak value of the inductor current	[A]
$I_o$	DC output current of the Boost converter	[A]
$I_{oB}$	Average output current at the limit of continuous conduction	[A]
$I_{oB,max}$	Maximum value of $I_{oB}$	[A]
$I_{o,max}$	Maximum value of the DC output current	[A]
$i_q$	Stator current in $q$ -axis	[A]
$I_s$	AC side rectifier input current	[A]
$J$	Moment of inertia of the wind turbine	[kgm <sup>2</sup> ]
$K$	Scale factor	
$L$	Inductance	[H]
$L_1$	Stator inductance	[H]
$L_{boost}$	Inductance of the Boost converter	[H]
$L_d$	Stator inductance in $d$ -axis	[H]
$L_{min}$	Minimum value of this inductance	[H]
$L_q$	Stator inductance in $q$ -axis	[H]
$m$	Output vector of the Synchronous Machine block	
$N$	Number of turns	
$n_r$	Rotor speed from the generator side	[rpm]

$n_s$	Synchronous speed	[rpm]
$n_{series}$	Number of semiconductors in series in the rectifier	
$n_{series,IGBT}$	Number of IGBT in series in the rectifier	
$n_{tr}$	Turbine rotor speed from the turbine side	[rpm]
$p$	Number of pole pairs	
$P_{cond,IGBT}$	Conduction losses in the IGBT	[W]
$P_{cond,rect}$	Conduction losses in the rectifier	[W]
$P_{copper}$	Copper losses in the inductor	[W]
$P_d$	Output power of the diode rectifier	[W]
$P_e$	Generated electric power	[W]
$P_{mec}$	Mechanical power given by the turbine	[W]
$P_o$	Output power of the Boost converter	[W]
$P_{switch,IGBT}$	Switching losses in the IGBT	[W]
$R$	Resistance	[ $\Omega$ ]
$R_a$	Armature resistance of the PMSG	[ $\Omega$ ]
$R_L$	Electrical resistance of the inductor	[ $\Omega$ ]
$R_r$	Rotor radius	[m]
$T$	Applied mechanical torque in the wind turbine	[Nm]
$T_e$	Electromagnetic torque	[Nm]
$t_f$	Fall time	[s]
$T_m$	Mechanical torque	[Nm]
$t_{off}$	Switch off duration	[s]
$t_{on}$	Switch on duration	[s]
$t_r$	Rise time	[s]
$T_s$	Switching time period	[s]
$U_d$	DC side rectifier voltage	[V]
$u_d$	Stator voltage in $d$ -axis	[V]
$U_{LL}$	rms line-to-line voltage	[V]
$U_o$	DC output voltage of the Boost converter	[V]
$u_q$	Stator voltage in $q$ -axis	[V]
$V_{IGBT}$	Off state voltage of the IGBT	[V]
$V_{on,diode}$	On state voltage in the diode	[V]
$V_{RRM}$	Maximum voltage that the device can block repetitively	[V]
$\alpha$	Angular acceleration	[m/s <sup>2</sup> ]
$\beta$	Pitch angle	
$\eta$	Efficiency of the converter	
$\mu_0$	Magnetic permeability of free space ( $4\pi \cdot 10^{-7}$ )	[H/m]
$\lambda$	Tip speed ratio	
$\rho$	Air density = 1.225	[kg/m <sup>3</sup> ]

$\rho_{core}$	Core material density	[g/cm <sup>3</sup> ]
$\rho_L$	Electrical resistivity of the inductor	[ $\Omega\text{mm}^2/\text{m}$ ]
$\Omega$	Rotational speed	[m/s]
$\omega$	Line frequency	[rad/s]
$\omega_r$	Rotor speed from the generator side	[rad/s]
$\omega_s$	Wind speed	[m/s]
$\omega_{tr}$	Turbine rotor speed from the turbine side	[rad/s]
$\psi$	Permanent magnet flux linkage	[Vs]
$\psi_{av}$	Average leakage flux in the inductor	[Wb turns]
$\Delta I_L$	Inductor current ripple	[A]
$\Delta_1 T_s$	Interval of time where the inductor current is decreasing to zero	[s]
$\Delta_2 T_s$	Interval of time where the inductor current is zero	[s]
$\Delta U_o$	Desired output voltage ripple	[V]

## Glossary

AC	Alternative Current
DC	Direct Current
EMF	Electromotive Force
EMSG	Electrically Magnetized Synchronous Generator
HVDC	High Voltage Direct Current
PCC	Point of common connection
PMSG	Permanent Magnet Synchronous Generator
rms	Root mean square value
WRSG	Wound Rotor Synchronous Generator



# 1 Chapter One

## Introduction

### 1.1 Problem overview

In the last years, the overall view of the power systems has changed. The classical systems are based on large power plants at right locations that produce the main part of the electricity and then, the electricity is transported to the consumption centres through long distance transmission lines. After that, the system control centres are responsible to guarantee the quality of the power. But the idea changed when the dispersed generation units started to increase: wind turbines, photovoltaic generators, small hydro, steam powered combined heat and power, etc. This has an influence on the grid and the control of the system.

Renewable energies have been taking an important role in this disperse generation. The advantages are the reduction of the harmful emissions and the permanent availability of the staples. Within these resources one of the most important and developed is the wind turbine technology, with turbines growing in size to nearly 5 MW.

Currently, one of the main problems that onshore wind power has is the limitation of spaces available to place the turbines. Considering, in addition, the better wind conditions and the less noise and visual impacts at the offshore locations, the developments are being moved to the sea. There are some other advantages [1]:

- Higher wind speeds (a 30 % more power production can be reach with a 10% increase in wind speed [2]).
- Less turbulence and large areas for bigger projects.
- Lower wind shear.

But there are also some disadvantages [1]:

- The more expensive marine foundations and the integration into the grid.
- The more expensive construction methods and access.
- The more limited access for maintenance.

Due to all of these extra costs necessary for the offshore wind power plants, the studies of the last years have been focused in new and cheap systems to generate, control and transport the electricity from the sea to the shore. The transmission is moving from AC current to DC due to the long distances between the offshore wind park and the network connection point, that is, generation of large amounts of capacitive current in the AC lines when the length of the cables increase. Also, HVDC gives the possibility to have more control on the energy transmitted and the components of the wind farm instead of the extra costs due to the large transformers needed for these voltage levels.

## **1.2 Previous work**

A comprehensive study about several configurations of large wind parks has been presented in [3], including investigations of energy losses, comparison of costs of the different configurations as well as possible control schemes and electrical grid limitations.

In [14] an investigation of generating systems for DC connected wind turbines is presented. Two DC generating systems were presented as well as a model of them and a suitable control.

In a previous Master Thesis [8] a design, control and simulation of an offshore wind park with three different converters has been expounded. Also a study of losses and efficiency was done. In [9] a study of a model of a wind turbine with a permanent magnets synchronous generator was conducted.

## **1.3 Purpose of the work**

As it was explained before, the transmission is moving from AC current to DC current in offshore wind parks remote-located due to the generation of capacitive current in the AC lines when the length of the cables increase, and also, HVDC gives the possibility to have more control on the energy transmitted and the components of the wind farm. In HVDC, the power flow is fully defined and controlled, exists higher capability per cable, less cable losses than in AC and is not affected by capacitive current generated in the cables.

The purpose of this work is to study a basic and robust system that could be suitable to use in applications where the wind turbines are connected to a DC link. Then, it could be possible to increase the efficiency of each wind turbine system of the wind farm and avoid larger transformers at the output.

The investigation has been carried out with simulations using MATLAB Simulink in steady state, and more specifically using the SimPowerSystem tool of this software.

In particular, a focus is to make a high DC-voltage (the cheapest and most efficient possible) with an Electrically Magnetized Synchronous Generator or Permanent Magnet Synchronous Generator with trapezoidal back EMF voltage, a diode rectifier, a DC-filter and a Boost converter.

## **1.4 Outline of the thesis**

In Chapter 2 a general overview of the energy conversion in wind turbines and the models used for the turbine and the generator are presented. Also briefly information about variable and fixed speed wind turbines, offshore wind farms and several possibilities of DC high voltage systems for wind applications.



In Chapter 3 all the design studies of the electrical system components and previous theory knowledge necessary to understand how the different devices used behave and operate are presented.

In Chapter 4 simulation studies are explained. The system specifications, that is, characteristics of the generator as well as the explanation about how the data of the turbine was calculated are presented. Also, some verification studies to check the viability of implementing the system proposed and how some of the devices behave are introduced at the beginning. After this, the design of the Boost converter is explained and the simulation results are shown.

In Chapter 5 the analytical studies as well as some calculations of losses and possible size of the Boost converter's inductor are presented.

Finally, in Chapter 6 the conclusions and future work are shown.

In the appendix it is available the MATLAB code used to simulate and calculate the losses in the system.

## 2 Chapter Two

### Applications of DC High Voltage in Wind Turbines

Today, a trend is that offshore installations are becoming more attractive compared to onshore installations. One of the possible reasons is the lack of space available for more onshore wind farms and also, the increasing concerns about the noise and visual impacts.

An important aspect is that offshore large wind plants need improvements in the transmission lines and the transformation centres. The advantages are higher wind speeds that lead into more generated power and less turbulence and bigger space to construct the wind park. Some of the main problems are that it is more expensive to build up the turbines and transport the energy to the shore. Also, the AC cables are not able to transport energy over a long distance and, due to this, the idea of DC high voltage as the transmission technology has been gaining strength.

In this section a general layout about different DC high voltage configurations for wind turbines and wind farms, as well as an introduction to the energy conversion of the turbines is given.

#### 2.1 Wind turbines

##### 2.1.1 Energy conversion of wind turbines

The most commonly used units are horizontal axis turbines. These ones consist of different parts: tower, rotor and nacelle.

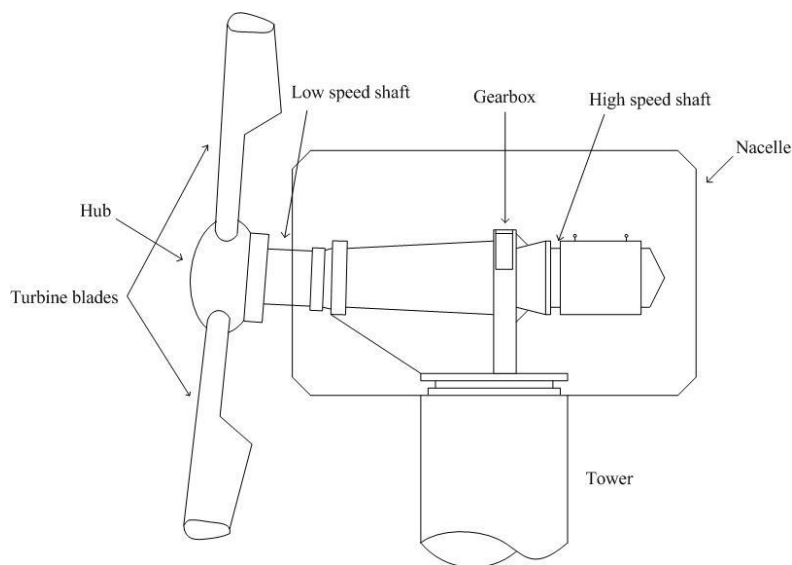


Figure 2.1: Wind turbine scheme.

The part that converts the energy of the wind into mechanical energy is the rotor. This energy is captured by the area swept by the rotor blades, and the efficiency of this conversion is a function of the pitch angle, tip speed ratio, air density and the shape of the blades [3]. The shaft, the hub and the blades form the rotor. The drive train, where the mechanical energy is transformed into electricity, is made up of a gear box, a generator and a rotor, but there exist some applications where a gear box is not used.

One classification of rotors that could be done is the following: constant pitch machines that cannot change the angle of the blades towards the rotor axis, and variable pitch machines which have this possibility. When the unit is working at high speeds, the energy extraction is to be controlled by the pitch angle [5]. There are also constant speed and variable speed generators.

In steady state, the conversion of the wind speed can be described with the following relations [3]:

$$P_{mec} = \frac{\pi\rho\omega_s^3 R_r^2}{2} C_p(\lambda, \beta) \quad (2.1)$$

$$\lambda = \frac{\omega_r R_r}{\omega_s} \quad (2.2)$$

### 2.1.2 Variable speed wind turbines

The fixed-speed turbines have a specific efficiency as a function of  $\omega_r$ , through that  $\lambda$  is uncontrolled. This means that at low wind speeds these machines do not work at maximum capacity. The advantage of the variable-speed units are that it is possible to obtain the maximum efficiency at lower rotor speeds, that means, maximum possible mechanical power output [3].

Other reasons to use variable speed are that there will be less stresses on the shaft and the fact that it is possible to control the reactive power. However, variable speed functionality complicates the generation of AC electricity at a constant frequency.

The synchronous generators used in variable-speed applications, that could have the fields separately excited or given by permanent magnets, give an output depending directly on the speed of the generator and the number of poles, quantified by [4]:

$$n_s = \frac{60f}{p/2} \quad (2.3)$$

## 2.2 Wind turbine and gearbox models

When the wind turbine rotor is rotating it achieves some angular momentum. In most of the applications it could be considered that the moment of inertia is constant. Then,

the product of the angular acceleration and the moment of inertia gives the torque applied [4]:

$$T = J \cdot \alpha \quad (2.4)$$

The rotating body of the turbine contains some kinetic energy expressed as:

$$E_k = \frac{1}{2} J \Omega^2 \quad (2.5)$$

Then, the power generated by the rotor of the generator is given by:

$$P_e = T \cdot \Omega \quad (2.6)$$

In case of a gearbox installed between the wind turbine and the generator, it has to be considered the speed ratio:

$$n_g = \frac{\omega_r}{\omega_{tr}} = \frac{n_r}{n_{tr}} \quad (2.7)$$

An interesting point to consider is that if the rotor is turning at some constant speed with a constant wind speed, the torque from the turbine rotor must be the same as the sum of the torque from the generator and loss torques in the drive train.

### 2.3 Model of the generator

In the paper [22] background theory about the PMSG model and control is explained. The following equations represent the dynamic model of the PMSG derived from the two-phase synchronous reference frame,  $d$ -axis is referred to the direction of rotation and the  $q$ -axis is  $90^\circ$  ahead the other. The theory of space vectors and the different transformations to other coordinate systems are widely explained in [21].

$$\frac{di_d}{dt} = -\frac{R_a}{L_d} i_d + \omega_r \frac{L_q}{L_d} i_q + \frac{1}{L_d} u_d \quad (2.8)$$

$$\frac{di_q}{dt} = -\frac{R_a}{L_q} i_q - \omega_r \left( \frac{L_d}{L_q} i_q + \frac{1}{L_q} \psi \right) + \frac{1}{L_q} u_q \quad (2.9)$$

The relation between the electrical rotating speed and the mechanical speed is:

$$\omega_r = n_p \omega_{tr} \quad (2.10)$$

In the simulations made in this thesis it will be considered that  $L_d = L_q = L_1$ , so then (2.8) and (2.9) can be transformed into [22]:

$$\frac{di_d}{dt} = -\frac{R_a}{L}i_d + \omega_r i_q + \frac{1}{L}u_d \quad (2.11)$$

$$\frac{di_q}{dt} = -\frac{R_a}{L}i_q - \omega_r \left( i_q + \frac{1}{L}\psi \right) + \frac{1}{L}u_q \quad (2.12)$$

The electric potential given by the flux of the magnets is [22]:

$$e_d = 0 \text{ and } e_q = \omega_r \psi = n_p \omega_r \psi \quad (2.13)$$

Finally, the electromagnetic torque can be calculated from (2.14) considering the assumption of the equal inductances on the  $d$ - and  $q$ -axes.

$$T_e = 1.5n_p i_q \psi \quad (2.14)$$

## 2.4 Offshore wind farms

During the last twenty years the interest in the offshore wind energy has been growing due to the advantages described in the first chapter.

To place an offshore wind farm some topics have to be considered: the required permissions, where are the shipping lines, environmental aspects related with birds migration, mammals, fishes, the seabed properties, water currents, transportation for maintenance, areas for construction, etc [4].

Also economic considerations interviewed with productivity have to be contemplated. Should the turbines be placed close together or keeping more distance between them? Should the wind farm be located near the coast or farther from shore where the wind speeds, and so the energy production, will be moderately high? If the decision leads to short distances, the installed costs will be less because the transmission cables to shore will be shorter and water depths are smaller, so the structures to support the turbines will be cheaper. To go deep on this topic reference [6] can be consulted.

## 2.5 DC connected wind turbines and high voltage systems

### 2.5.1 General view of wind parks

Generally, wind parks are made up of a certain number of single wind turbines, all of them connected to the collecting point by the local wind turbine grid. In this point, the voltage is increased to reach admissible values to transport the energy through the transmission system. At the end of it, the wind park grid interface is placed and is the element responsible to adapt the characteristics of the power, that is, voltage, frequency and reactive power, to the levels of the power demanded by the grid in the point of common connection (PCC) [3]. The structure of the park can be observed in Figure 2.2.

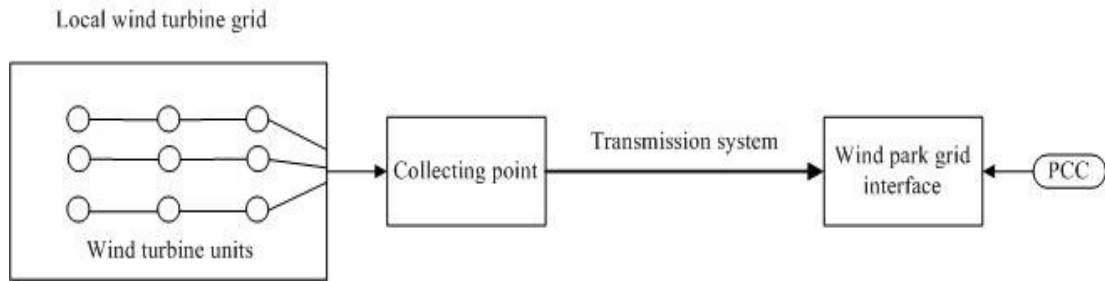


Figure 2.2: General functional scheme of a wind park.

A possible distance between the turbines is 7 rotor diameters in both directions. In the wind direction special cares must be considered. When the wind passes through the rotor it gets turbulent, so if the distance between the turbines is not big enough the wind increases the turbulence from the beginning until the end of the wind farm. These problems could lead to aerodynamical stresses and also, energy losses if the turbines are located close to each other.

## 2.5.2 Offshore system configurations

### 2.5.2.1 AC/AC

This system is suitable for small wind farms with short transmission distances. It follows the same structure shown in Figure 2.2. But if a higher voltage is desired, for large AC wind parks, it is necessary to install an offshore platform for the transformer and switch gear. This platform would be placed at the collecting point position.

### 2.5.2.2 AC/DC

In this system the transmission is using DC. When the PCC is far enough, it should be better to transport the power DC to avoid the problem of the reactive generated in the AC lines. The configuration is the same as the AC/AC, but here, instead of the transformer, an offshore converter station that allows control of the voltage and the frequency of the local AC wind turbine grid is placed. Then, the total efficiency can be increased.

### 2.5.2.3 DC/DC

The topology of this system is the same as the small AC wind park, but here each wind turbine has a rectifier. Therefore, the collecting point receives the power in DC form from the turbines and then, directly it is transported by the transmission system. At the wind farm grid interface an inverter for a proper connection to the PCC is installed.

The large DC wind farm configuration can be different than the large AC parks. If the output power of the turbines is high enough (20-40kV) only one transformation step is needed, if not (5kV) two steps are necessary [3].

On the other hand, to skip the extra costs and losses that the two transmission steps mean, the wind turbines can be connected in series together (Figure 2.3). Then, a suitable voltage for the transmission could be obtained directly, and big transformer offshore platforms are not required. The voltage insulation in each turbine is made by the local converters, and then, they should be able to operate at high voltage levels and, in case of failure of one of the turbines, the rest of them have to compensate the lack of power.

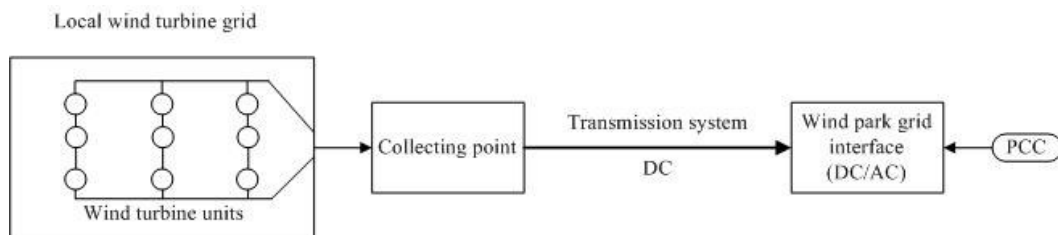


Figure 2.3: DC system with series wind turbine connected.

In the present work, the main goal is to provide these suitable voltages for transmission mentioned above at low speeds, using the individual rectifiers of each turbine and adding a step-up converter to rise up the voltage level. Then a smaller transformer at the collecting point could be suitable, and the efficiency at low wind speeds could be increased. It is supposed that at high wind speeds, close to rated operating points, the system is efficient enough and the use of these converters is less necessary.

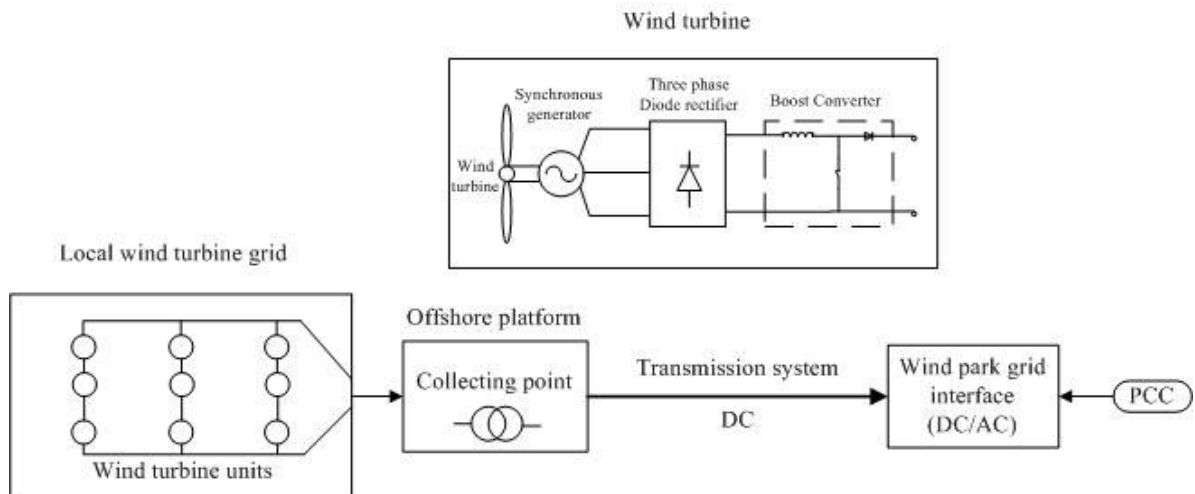


Figure 2.4: DC system purposed in this Thesis.

### **2.5.3 High voltage DC transmission**

In the last years, the size and use of offshore wind turbines have been increasing. Due to that, the distances to the shore are longer, often around 50-100km considering distance to shore and to the suitable connection point [16], and one of the possible solutions could be the type of transmission system. If the wind park is situated far from the shore and is big enough, HVDC transmission system could be needed.

There are two technologies involved in the HVDC transmission technology: Line Commutated Converters (LCC) and the Voltage Source Converters (VSC).

The first one, also called HVDC classic, is the traditional HVDC system. It uses thyristor based converters, that cannot be turned off unless the current through them reverses. The main losses exist at the ends of the cable, in the converters [16].

The other one is a new technology based on converters that use IGBT modules. The main advantage is that this system can absorb and supply reactive power if it is necessary, so it can contribute in the control of the system. The main losses occur as the LCC, at the converters, due to the high switching losses.

More information about HVDC and high voltage transmission systems can be obtained from the references [17, 18, 19, 20].



## 3 Chapter Three

### Electrical System Components

In the previous chapters some of the main questions concerning the DC wind turbines systems have been set out. This project tries to achieve a possible solution to some of them, studying a low-cost system and its efficiency, so in the following chapter a brief explanation of the components of the system is carried out.

#### 3.1 Why synchronous generator?

The synchronous generator, compared with the induction generator, is more complicated from the mechanical point of view and more expensive. But its main advantage is that excitation current to magnetize the machine is not needed [2], and thus, higher power factor and efficiency can be achieved.

There are different ways to create the magnetic field in the synchronous machines. It could be done by using a field winding (EMSG or WRSG) or by permanent magnets (PMSG).

The synchronous generator normally needs the use of power electronic converters, so it is more suitable when a full power control is required. That is the reason why these machines are widely used in variable-speed wind applications or on large grid-connected turbines.

#### 3.2 System topology

The wind turbine system suggested is shown in Figure 3.1. The different basic components can be observed: the wind turbine, the synchronous generator, a three phase diode rectifier and a boost converter.

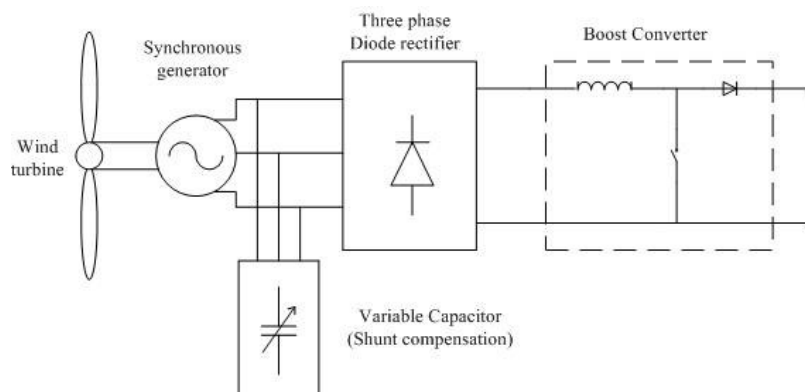


Figure 3.1: System topology.

### **3.2.1 Wind turbine**

In most of the wind turbine units exists a gear box between the turbine and the generator to step up the speed and reduce the torque, that is, reduce the current. This leads to the possibility of using a smaller machine.

### **3.2.2 Electrically magnetized synchronous generator**

The EMSG is commonly named wound-rotor synchronous generator (WRSG) and in large central station power plants it is widely used. In variable-speed wind turbine applications is used with power electronic converters.

The rotor winding of the synchronous machines is excited with DC current using slip rings and brushes, or with a brushless exciter with a rotating rectifier [2]. In both cases the current is externally controlled. The exciter has its output on the rotor, its field is rather stationary, and it fed directly into the field windings. The exciter field created is rotating at synchronous speed, and then, the speed of the synchronous generator is calculated with the frequency and the number of pole pairs according to (2.3).

### **3.2.3 Permanent magnet synchronous generator**

The use of the PMSG for wind turbine applications has increased in the last years [4]. Now it is the main choice for generators in small wind turbines and some in the large ones as well.

The main advantages are that no energy supply is needed to excite the machine and power can be generated at any speed. The magnetic field is provided by the permanent magnets, usually integrated into a salient poles rotor or cylindrical rotor. Brushes, slip rings or commutator are not needed, and the simplicity of the machine make this generator quite rugged [4]. The only difference between the PMSG and the rest of the synchronous generators is that permanent magnets provide the field instead of electromagnets.

Additionally, in comparison with the EMSG, the gearless PMSG is more efficient under partial load [13], the energy cost per kWh is lower [13], is lighter (EMSG needs more mass in the copper) and has less copper losses due to permanent magnets have smaller pole pitch and there is no rotor winding [14].

However, the use of permanent magnets has some disadvantages. One is the increasing costs due to the materials used for constructing the magnets. In addition, a power converter is required in order to control the generating voltage and frequency levels and adjust them in balance with the voltage and frequency of the transmission system [2].

### 3.2.4 Diode rectifier

Power converters have an important role in wind energy systems and are being used more frequently as the technology develops and the costs increase. These devices are used to change the form of the electrical power, AC to DC, or the frequency and voltage levels. In most of the applications, the input is a 50- or 60-Hz sine wave AC voltage and the trend is to use cheap rectifiers with diodes where the power flow can only flow from the AC side to the DC side [7].

Inside the group of the power converters, the rectifiers are the devices that convert the power from the AC form into the DC form. For systems with a power output higher than 15 kW, three-phase or poly-phase diode rectifiers should be employed [12].

#### 3.2.4.1 Three-phase full bridge diode rectifier

These rectifiers have the highest possible transformer utilization factor for a three-phase system, so, due to that, they are frequently used in high power applications. In Figure 3.2 a three-phase, six-pulse, full bridge diode rectifier is shown.

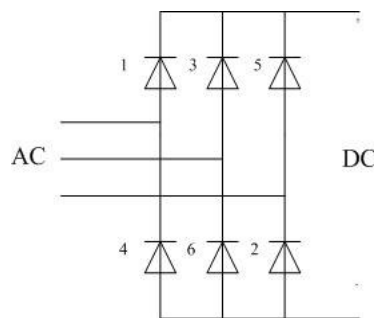


Figure 3.2: Three-phase diode-bridge rectifier.

As it is an uncontrolled converter, the three-phase line currents generated by the SG cannot be regulated by this object. So, after the diode rectifier, a device that allows some kind of control over the machine have to be installed.

There are some improvements that could be done to optimize the operation of this device. They are shown in Figure 3.3.

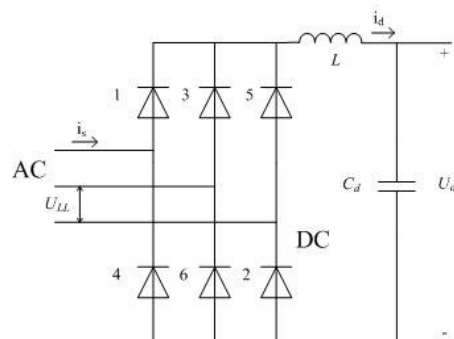


Figure 3.3: Three-phase diode-bridge rectifier with  $L$  and  $C_d$ .

One of them, could be the possibility of connecting a large capacitor on the DC side,  $C_d$ , to work as a filter and obtain a DC output voltage as ripple free as possible. The main problem is that it generates current harmonics.

Another thing to consider is that in diode rectifiers with small  $L$ , the current  $I_d$  are highly discontinuous, then, the rms of the input current  $I_s$  becomes large and the power is drawn from the utility source at a very poor power factor. The minimum value of this inductance required to make the current continuous and can be calculated with the following equation:

$$L_{\min} = \frac{0.013U_{LL}}{\omega I_d} \quad (3.1)$$

Also, with a continuous  $I_d$  flowing, the average value of the output voltage can be calculated with the following expressions [7]:

$$A_d = \int_{-\pi/6}^{\pi/6} \sqrt{2}U_{LL} \cos \omega t \cdot d(\omega t) = \sqrt{2}U_{LL} \quad (3.2)$$

$$U_d = \frac{A_d}{\pi/3} = \frac{3\sqrt{2}}{\pi}U_{LL} = 1.35U_{LL} \quad (3.3)$$

The equation used for the average value (3.2) is derived from Figure 3.4 [15].

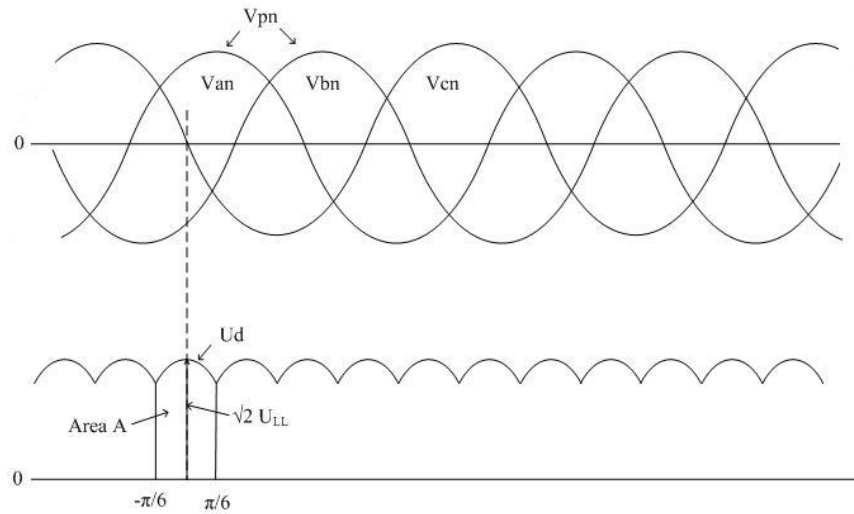


Figure 3.4: Three-phase rectifier voltage waveforms with continuous  $I_d$ .

Finally, if  $L$  is large enough to make  $I_d$  practically constant, the power factor obtained is close to 0.95 [7].

### 3.2.5 Boost converter

This converter is included in the group of the DC-DC converters, where the average DC output voltage must be controlled and made equal to a desired level.

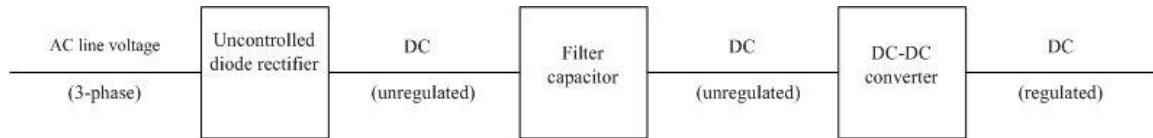


Figure 3.5: DC-DC converter system.

The switch-mode DC-DC converters use a number of switches to transform the level from one DC value to another. So, in the case of a given input voltage, the average output can be controlled by controlling the switch on and off durations ( $t_{on}$  and  $t_{off}$ ). These devices can operate in two different modes: continuous-current conduction and discontinuous-current conduction [7].

Figure 3.6 shows the topology of the Boost converter or the step-up converter, as it is commonly known.

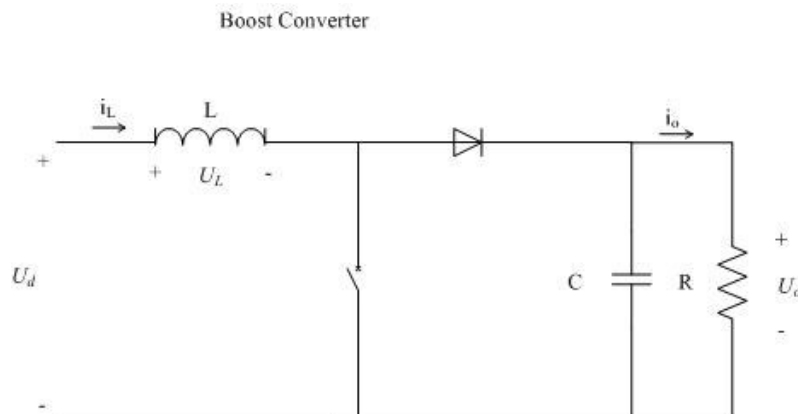


Figure 3.6: Boost converter (dc-dc).

The step-up converter is normally used in regulated DC power supplies, and the input voltage is always lower than the output voltage. Its operation mode is easy to understand. When the switch is on, the load is isolated because the diode is reversed biased. In this moment, the source of energy situated at the input charges the inductor. When the switch is off, the diode conducts normally and the load receives the energy from the input and the inductor at the same time. In this thesis the analysis are in steady-state, so the output filter should be very large to guarantee that the output voltage  $U_o$  remains constant [7].

The Boost converter has continuous input current, so a smaller capacitance between the diode rectifier and the converter is needed compared to other converters with discontinuous input current. With this device it is possible to have a control over the current flowing to the different loads.

### 3.2.5.1 Continuous conduction mode

In this mode, the inductor current flows continuously, that is,  $i_L(t) > 0$ .

In steady-state the time integral of the inductor voltage over one period must be zero as it is shown on (3.4) [7]:

$$U_d t_{on} + (U_d - U_o) t_{off} = 0 \quad (3.4)$$

Then, it can be rewritten as follows [7]:

$$\frac{U_o}{U_d} = \frac{T_s}{t_{off}} = \frac{1}{1-D} \quad (3.5)$$

Assuming no losses in the circuit [7]

$$U_d I_d = U_o I_o \quad (3.6)$$

and then:

$$\frac{I_o}{I_d} = (1-D) \quad (3.7)$$

It is necessary to establish the boundary between both modes of operation, continuous and discontinuous mode. In the continuous one, by definition,  $i_L$  reach zero value at the end of the off interval. The average value at this point, using in the last step, (3.5), can be expressed as

$$I_{L,\lim} = \frac{1}{2} i_{L,\text{peak}} = \frac{1}{2} \frac{U_d}{L} t_{on} = \frac{T_s U_o}{2L} D(1-D) \quad (3.8)$$

Using (3.7) and (3.8), and considering that the input and output current across the inductor is the same, then the expression of the output current in the limit of the continuous conduction mode is obtained:

$$I_{oB} = \frac{T_s U_o}{2L} D(1-D)^2 \quad (3.9)$$

### 3.2.5.2 Discontinuous conduction mode

Now, it is assumed that  $U_d$  and  $D$  remain constant as the output power is decreasing. Due to that, there is a lower  $I_d$ . In both modes of operation the value of  $i_{L,\text{peak}}$  is the same, so a discontinuous mode is only possible if  $U_o$  rises up in Figure 3.7b.

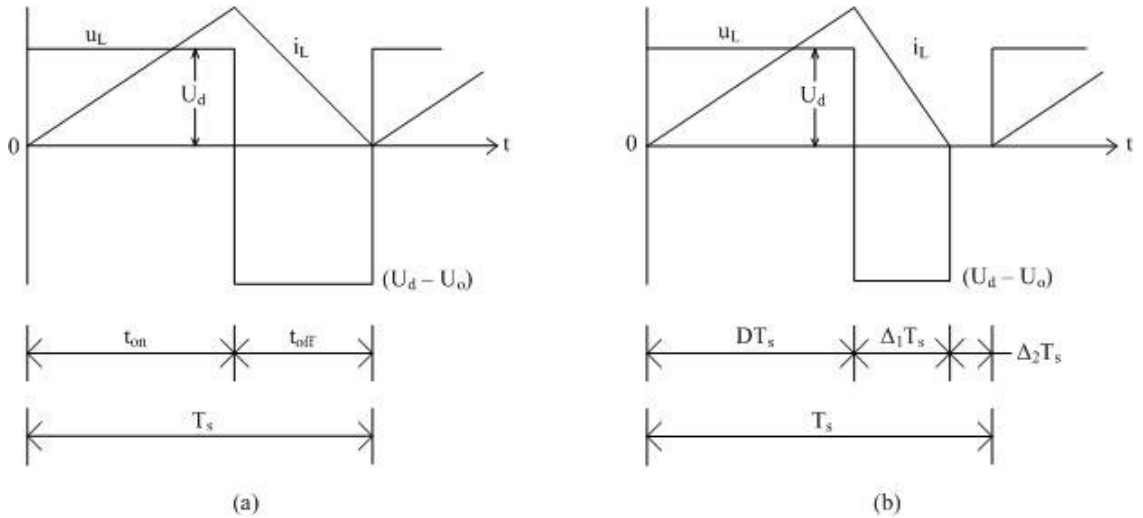


Figure 3.7: (a) boundary of continuous/discontinuous conduction, (b) discontinuous conduction.

Integrating the inductor voltage over one time period, as it has been done in the continuous mode [7],

$$U_d DT_s + (U_d - U_o) \Delta_1 T_s = 0$$

$$\frac{U_o}{U_d} = \frac{\Delta_1 + D}{\Delta_1} \quad (3.10)$$

and considering that  $P_o = P_d$ , then

$$\frac{I_o}{I_d} = \frac{\Delta_1}{\Delta_1 + D} \quad (3.11)$$

Observing Figure 3.8b, the average of the input current can be expressed as follows [7]:

$$I_d = \frac{U_d}{2L} DT_s \cdot (D + \Delta_1) \quad (3.12)$$

Now, operating with (3.11) and (3.12):

$$I_o = \left( \frac{T_s U_d}{2L} \right) D \Delta_1 \quad (3.13)$$

In practise, and using (3.10), (3.13) and another approximated equation (3.14), it is possible to express  $D$  as a function of the load current [7]:

$$I_{oB,\max} = 0.074 \frac{T_s U_o}{L} \quad (3.14)$$

$$D = \left[ \frac{4}{27} \left( \frac{U_o}{U_d} \right) \left( \frac{U_o}{U_d} - 1 \right) \frac{I_o}{I_{oB,max}} \right]^{1/2} \quad (3.15)$$

In the design of the step-up converter it has to be considered that in this mode of operation, if the output voltage is not controlled in each switching period, some energy is transferred from the input to the load and the capacitor. Then, if this load cannot absorb this energy, the output voltage, that is the same as the voltage across the capacitor, will increase until an energy balance is established. Due to this higher output voltage, the capacitor could breakdown if the load is very light.

### 3.2.6 Variable capacitor

In the system proposed at the beginning of this chapter, if only the diode rectifier is installed, the PMSG cannot keep the voltage in phase with the current. That leads to a voltage drop over the generator inductance and a low output power. As the DC voltage varies with the speed of the generator and the load, some reactive compensation in order to increase the quality of the output power could be necessary.

One option could be a shunt reactive power compensation, see Figure 3.1 at the beginning of the chapter, but the main disadvantage is that these capacitors give more reactive power at no load and less at heavily loaded conditions. For this reason it is better to use a series compensated capacitor shown in Figure 3.8.

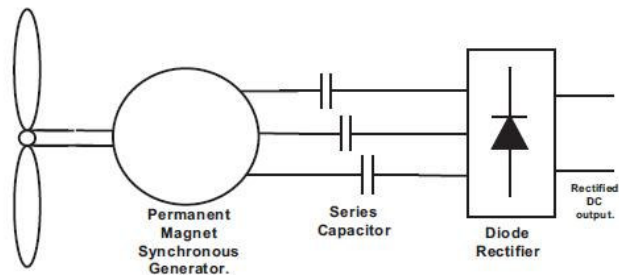


Figure 3.8: PMSG with series compensation.



## 4 Chapter Four

### Simulation Studies

All the simulations presented in this report were carried out with the SimPowerSystems software. It operates in the MATLAB Simulink environment and it is a tool that allows the user to easily and rapidly build up models to simulate power systems. More information can be found at [10].

In this chapter some of the SimPowerSystem blocks used in the simulations are explained, as well as the structure of the main system studied in the Simulink environment.

In all the different configurations that can be found in the following sections, the speed of the PMSG is considered to be constant because, in the time scale of the dynamics of the system, the mechanical time constants are higher than the electrical time constants.

#### 4.1 SimPowerSystems

SimPowerSystems is a software included in the MATLAB Simulink environment, so extensive documentation about the different blocks and how to use them at the MATLAB Help folders can be found. Nevertheless, some briefly explanation of the units used in the simulations of this thesis is given in the next sections.

##### 4.1.1 Permanent magnet synchronous machine block

This block can operate in two different modes, generator or motor, depending on the sign of the mechanical torque. When the speed is positive, a positive torque signal indicates motor mode and a negative signal indicates generator mode. The dynamic model used by MATLAB is similar than the one proposed in [21], so for more information this book can be consulted.

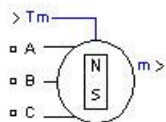


Figure 4.1: Permanent Magnet Synchronous Machine Simulink block.

In the Dialog Box and Parameters different conditions and values for the machine like the back EMF waveform, the type of input ( $T_m$  and  $\omega_r$ ) or the stator inductances and resistance can be chosen.

The output of this block is a vector named  $m$  containing 13 signals (stator currents, rotor speed, rotor angle, electromagnetic torque, etc) that can be demultiplex by a Bus Selector block [10].

Also it has to be considered that the Permanent Magnet Synchronous Machine block assumes a linear magnetic circuit with no saturation of the rotor and stator iron, due to the large air gap normally used in these machines.

### 4.1.2 Universal Bridge block

This device is part of the power electronics library inside SimPowerSystems. With this block, a three-phase converter can be implemented, and it consists of six power switches connected in a bridge configuration [10]. The type of converter can be selected in the dialog box (diode, thyristor, GTO, IGBT, MOSFET and ideal switch):

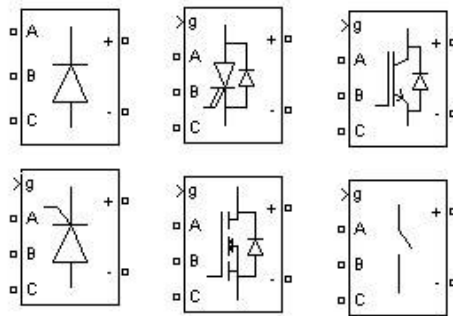


Figure 4.2: Different possibilities of the Universal Bridge Simulink block.

In the dialog box also it is possible to choose the number of legs of the bridge, and the parameters of the snubber circuit if it is needed. It is possible to allow measurements in the block, such branch current and terminal voltages, so the behaviour of the device can be followed.

### 4.1.3 More blocks used in the simulations

There are some other blocks from SimPowerSystems that have been used in the simulations, but only briefly information about them is needed.

The inductors, resistors and capacitors used are all coming from the Series RLC Branch block. The appearance of this device could be observed in Figure 4.3. As other elements of this Library, the type of branch, including simple elements like an inductor or a capacitor can be chosen. Also, it is possible to select the initial values and the desired measurements.



Figure 4.3: Series RLC Branch Simulink block.

The switch of the Boost converter has been implemented using the Ideal Switch block. It is not really a physical device, the switch is simulated as a resistor in series with a switch controlled by a logical signal called  $g$  as it can be seen in Figure 4.4. When  $g > 0$  the Switch turns on, if  $g = 0$  it turns off. The voltages and currents across the Switch can be measured if the measurement points are activated.

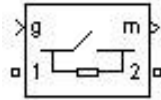


Figure 4.4: Ideal Switch Simulink block.

Another block used is the Diode. It is a semiconductor device that is controlled by its own voltage and current, from anode to cathode. When it is forward biased, it starts to conduct with a small forward voltage, close to zero. When the current across the device becomes zero, then it turns off, and it remains in this position while the diode is reversed biased, that is, when the voltage over it is negative [10].

The Diode block is simulated by a resistor, an inductor, and a DC voltage source connected in series with a switch. Also a snubber circuit is available if it is necessary.

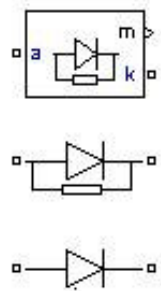


Figure 4.5: Diode Simulink block.

The last important block is the Multimeter. It is used to measure currents and voltages in some parts and elements of the system, that ones where the measurement point is activated.

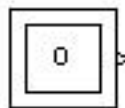


Figure 4.6: Multimeter Simulink block.

## 4.2 The system specifications

In this section, the characteristics of some of the devices that are necessary to specify in order to start the simulations are expounded. Also, data inputs to the wind turbine are presented, originally from the measurements done in the reference [11], where a previous study of a wind turbine was carried out, and are shown in two graphics, Figure 4.7 and Figure 4.8.

### 4.2.1 Characteristics of the wind turbine

In the simulations, the gear box was not considered as an element of the system, only to calculate the speed inputs to the generator that are the different values of  $\omega_r$ . The turbine and the data used during the simulations are taken from the project of the reference [11].

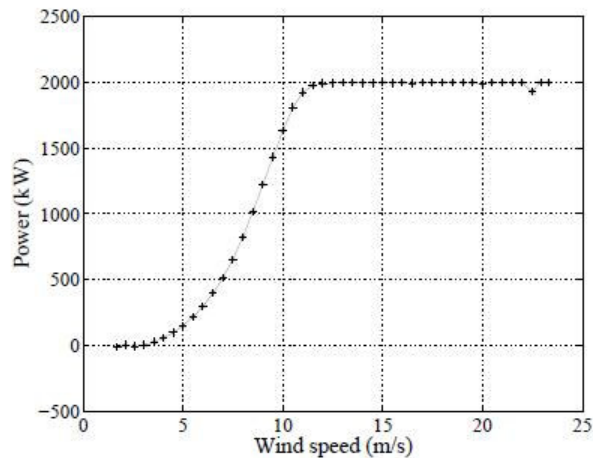


Figure 4.7: Electric power as a function of wind speed, averaged results [11].

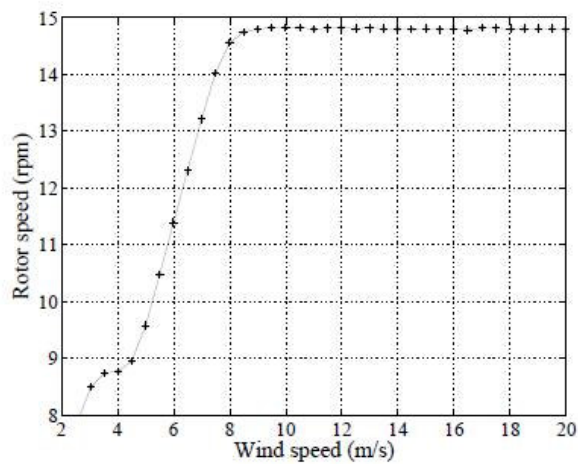


Figure 4.8: Rotor speed as a function of wind speed, averaged results [11].

From these two figures, the operating points were selected, that is, rotor speed and electric power, corresponding with some of main wind speeds (4, 5, 6, 8, 10, 12 m/s). These data were used as the inputs of the generator.

*Table 4.1 Data from the Figure 4.7 and Figure 4.8*

Wind speed [m/s]	Rotor Speed [rpm]	Electric power [kW]
4	8.7	100
5	9.6	225
6	11.4	350
8	14.6	800
10	14.8	1650
12	14.8	2000

Characteristics of the turbine:

- Cut-in wind speed: 4 m/s
- Gearbox speed ratio:  $n_g = 113.5$
- Rated wind speed: 12 m/s

#### **4.2.2 Characteristics of the generator**

The generator is a PMSG with the following characteristics:

- Armature resistance:  $R_a = 100 \text{ m}\Omega$
- Stator inductance:  $L_1 = 1.5 \text{ mH}$
- Pole pairs:  $n_p = 4$
- Rated power: 2 MW
- Rated voltage: 5 kV
- Rated frequency: 100 Hz
- Flux linkage:  $\psi = 6.5 \text{ Wb}$  [calculated with the equation (2.13)]

- Electrical rotating speed:  $\omega_r = \frac{2\pi f}{n_p}$ , at rated operation is  $\omega_r = 157.08$  rad/s

### 4.3 Verification studies

In this section of Chapter 4, studies to prove if some of the simple elements purposed on the system work properly were done, and also if the simulations match the expected results.

#### 4.3.1 Calculation of the generator output voltage values

First of all, to be able to calculate the different values of the Boost converter duty cycle, it is necessary to obtain the line-to-line voltages at the output of the generator. Then, it can be possible to continue checking if the rectifier works properly and after that follows to implement the whole system and investigate the behaviour of the step-up converter.

In Figure 4.9, the system used to calculate these voltage values at several wind speeds is shown.

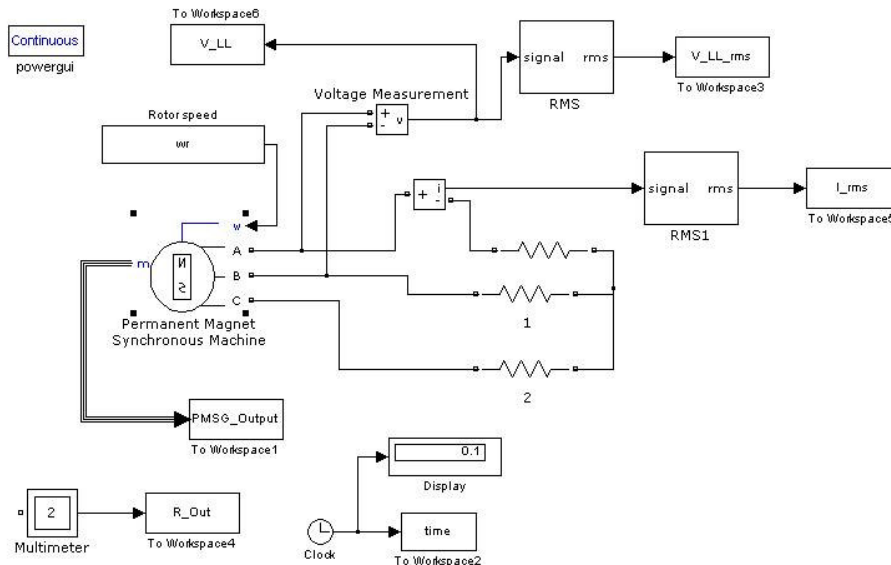


Figure 4.9: Simulink file with PMSG and a three-phase resistance load.

In Table 4.2, the measured values of the line-to-line output voltage of the generator are recorded. As it could be observed in Figure 4.9, the Voltage Measurement Simulink block is used to transform the electrical or measured signal into a Simulink signal. Then, the RMS block displays the rms value of this input signal. For more information about how these two Simulink blocks work consult [10].

In order to check if the simulation of the different operation points are done properly, the theoretical electromagnetic torque, (4.1), is compared with the one given by Simulink. To illustrate how the values are taken from the graphics, in the following figures are plotted containing some of the relevant signals of the rated operation point, that is, wind speed of 12 m/s. The figures resulting from the other operating points are not shown in the report but can be implemented following the MATLAB code provided in the appendix.

$$T_e = \frac{P_e}{\omega_r} \quad (4.1)$$

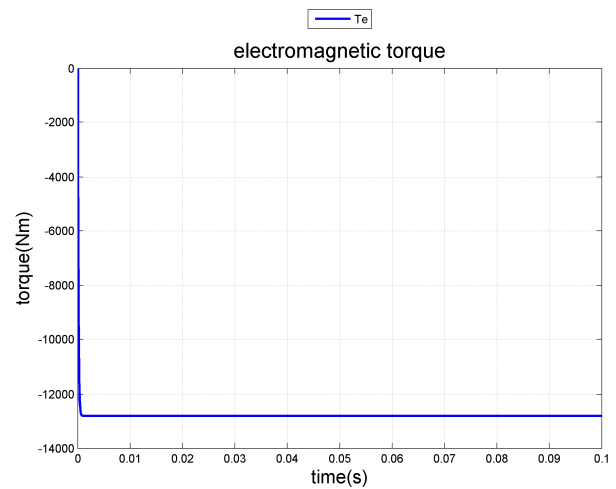
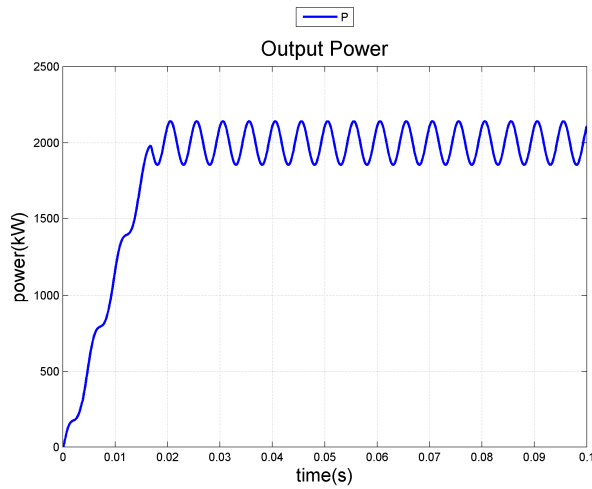


Figure 4.10 and 4.11: output power and electromagnetic torque at rated values ( $\omega_s = 12$  m/s).

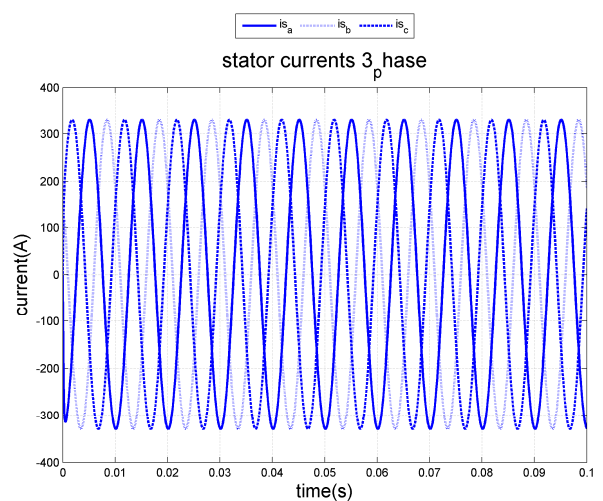
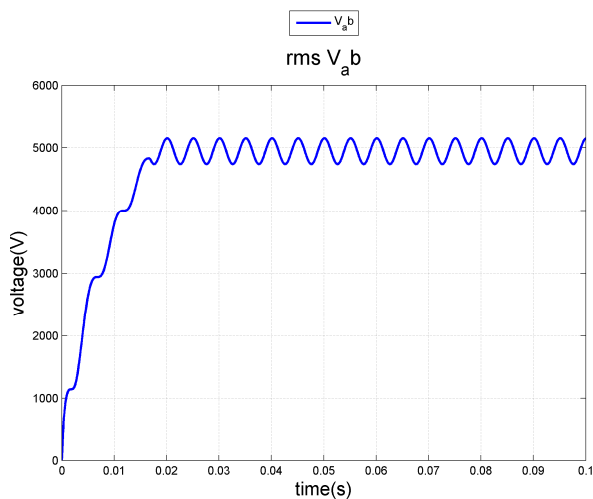


Figure 4.12 and 4.13: rms value of the line-to-line voltage and the three-phase stator currents at rated values ( $\omega_s = 12$  m/s).

Table 4.2 Data table with the final values of the PMSG line-to-line voltage

Wind speed $\omega_s$ [m/s]	Rotor Speed $n_r$ [rpm]	Electric power $P_e$ [kW]	$U_{LL}$ [V]	$T_e$ [Nm]
4	8.7	100	2935	1083
5	9.6	225	3230	2208.3
6	11.4	350	3840	2892.7
8	14.6	800	4900	5162.8
10	14.8	1650	4950	10504
12	14.8	2000	5000	12732

Taking the mean value of the electromagnetic torque signal given by the simulations and comparing with the theoretical value calculated it can be concluded that the implementation of the system works properly, and then, the values of the line-to-line voltage measured can be considered right for the following simulations.

### 4.3.2 Three-phase full bridge diode rectifier

In Figure 4.14 the Simulink scheme used in the verification of the diode rectifier can be observed, using a small inductor and a DC Voltage Source block working as a battery that will be charged with the energy generated by the PMSG and transmitted through the diode rectifier. The objective of this implementation is to check if the rectifier is working properly. It can be done comparing the voltage level at the output of the device given by the simulations with the calculated values given by the theory, for example (3.3) and the values of  $U_{LL}$  obtained in the previous section, listed in Table 4.2.



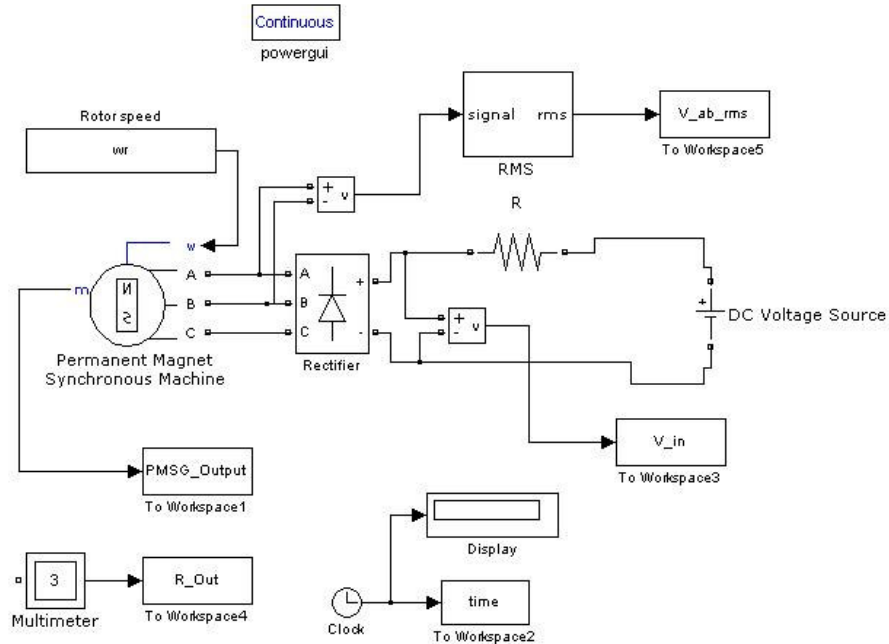


Figure 4.14: Simulink file with the PMSG, the rectifier and the DC Voltage Source.

As it can be observed in the following figures, this system is not valid for the purpose that was suggested. The output power oscillates a lot because it is a function of the rectifier output voltage and current. As the current is highly discontinuous and almost zero the output power signal is not the correct one.

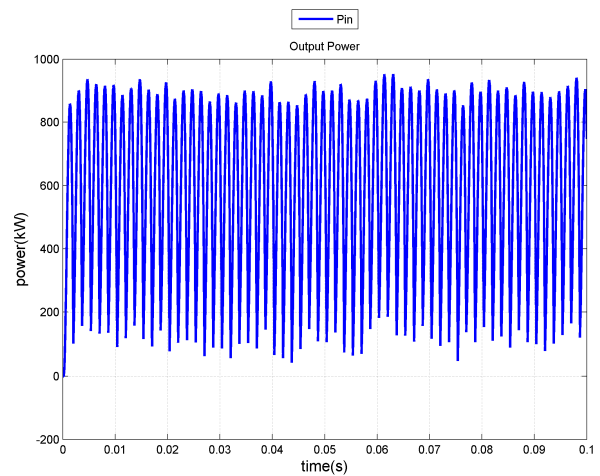
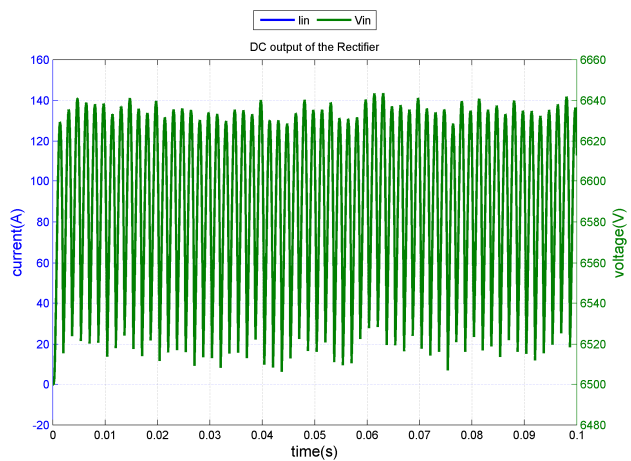


Figure 4.15 and 4.16: rectifier output voltage, current and power at rated values ( $\omega_s = 12 \text{ m/s}$ ).

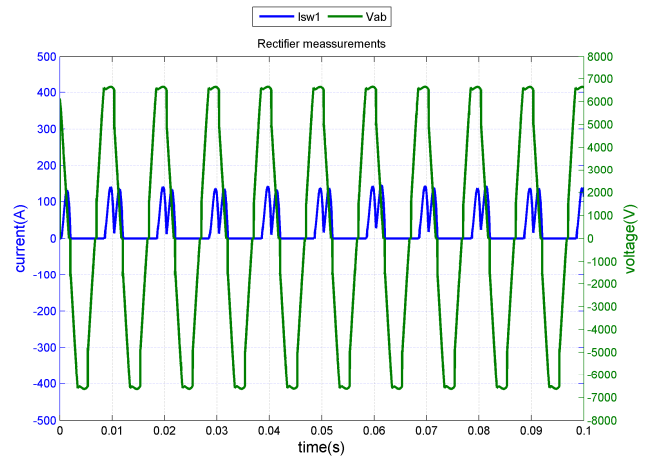
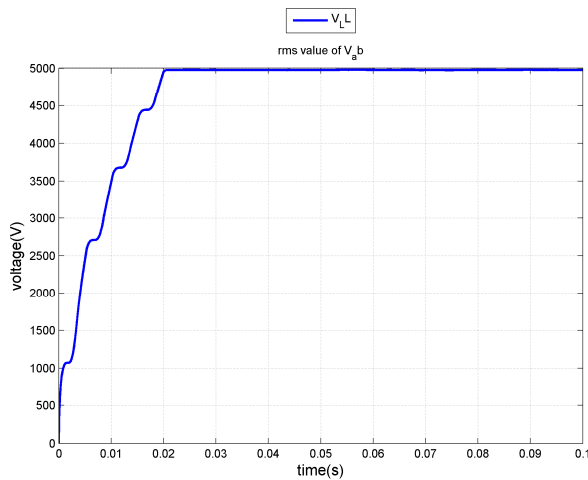


Figure 4.17 and 4.18: rms value of the line-to-line voltage and rectifier measurements at rated values ( $\omega_s = 12$  m/s).

The rectifier measurements refer to the current across one of the diodes that make the bridge and the line-to-line voltage at the output of the generator, that is, at the input of the rectifier. It can be observed that this last value is exactly the peak value of the line-to-line voltage.

The problem could be located at the DC Voltage Source used. This SimPowerSystems block is an ideal voltage source and only the voltage across this device can be measured, neither the current nor the power. The output power is the product of the voltage and the current across the resistor which was placed in the system in order to be able to measure this current. The DC source is setting some voltage level, approximately the same than the expected at the rectifier output, so it is making the current dropping with the consequence of lower power values. Also there is a large ripple due to the high ripple in the electromagnetic torque of the generator.

In the other points of operation the results of this topology are as bad as the rated ones. Due to this, it was decided to implement a new circuit to be able to check the functionality of the rectifier, Figure 4.19.

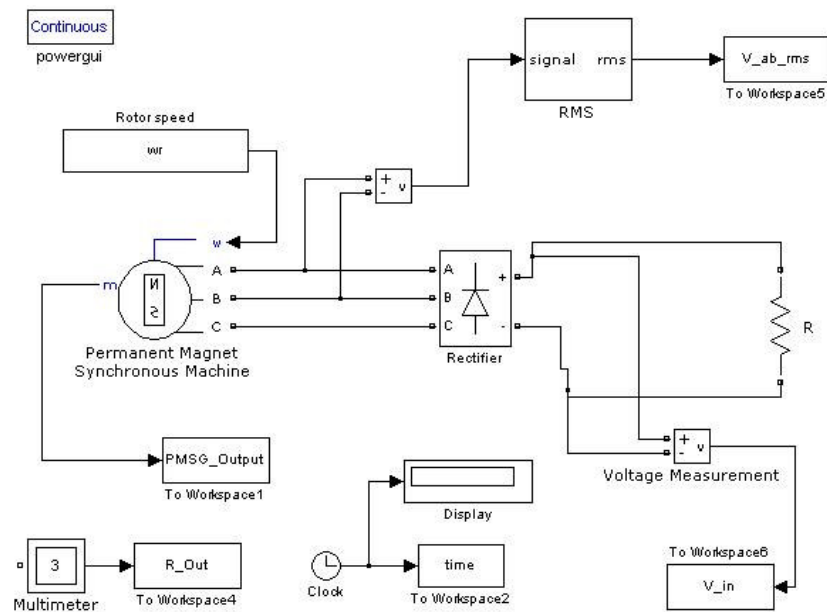


Figure 4.19: Simulink file with the PMSG, the rectifier and a load resistance.

The values of the resistance and the measured rectifier output voltages are presented in Table 4.3. As the output is in DC, (4.3) can be used to calculate the resistance:

$$P_e = U_d I_d \quad (4.2)$$

$$R = \frac{U_d^2}{P_e} \quad (4.3)$$

Table 4.3 Data used to simulate the turbine and voltage levels rectified

Wind speed $\omega_s$ [m/s]	Rotor Speed $n_{tr}$ [rpm]	Electric power $P_e$ [kW]	$T_e$ [Nm]	$U_{LL}$ [V]	$U_d$ [V] (theory)	$R$ [ $\Omega$ ] (theory)
4	8.7	100	1083	2935	3962.3	156.9982
5	9.6	225	2208.3	3230	4360.5	84.5065
6	11.4	350	2892.7	3840	5184	76.7824
8	14.6	800	5162.8	4900	6615	54.6978
10	14.8	1650	10504	4950	6682.5	27.0641
12	14.8	2000	12732	5000	6750	22.7813

In the next figures some results at different operating points are shown to prove that the theoretic output voltage values of the rectifier are almost the same than the ones simulated. Now, it is easy to check if the rectifier block is working as expected or not, in order to continue implementing the whole system. Then, in case of failures in the total system, it can be guaranteed that these errors are not coming from the rectifier or the generator, and it can be possible to focus on the Boost converter.

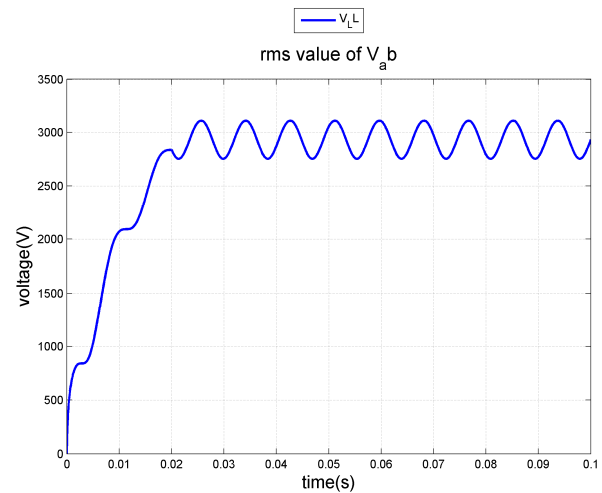
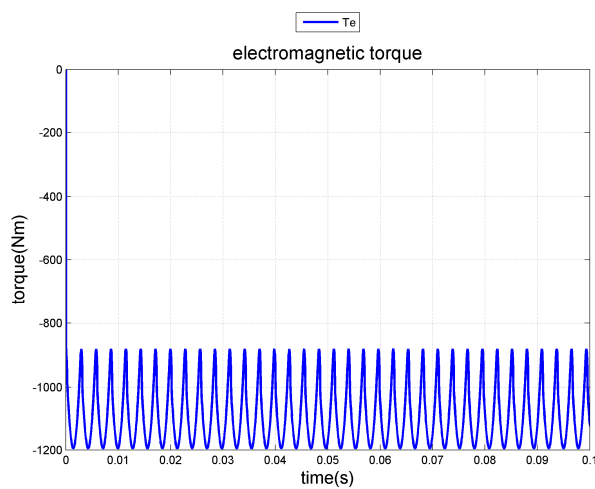


Figure 4.20 and 4.21:  $T_e$  and rms value of  $U_{LL}$  at  $\omega_s = 4$  m/s.

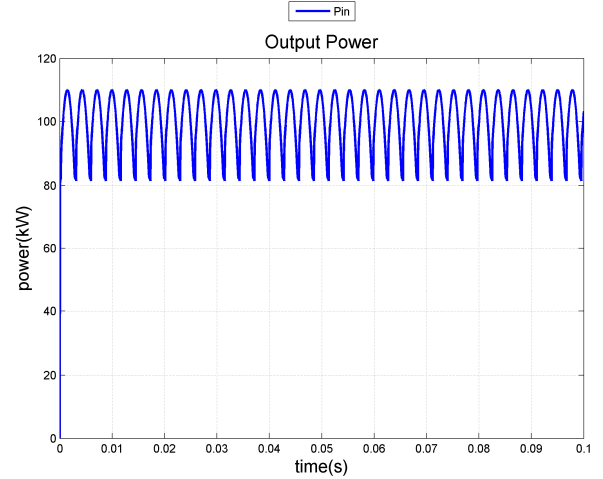
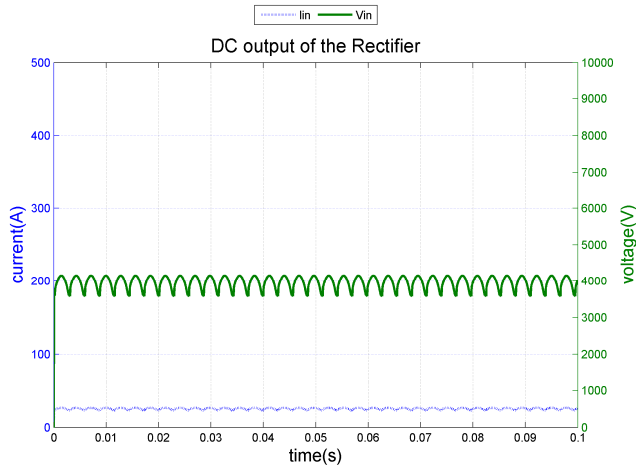


Figure 4.22 and 4.23: rectifier output voltage, current and power at  $\omega_s = 4$  m/s.

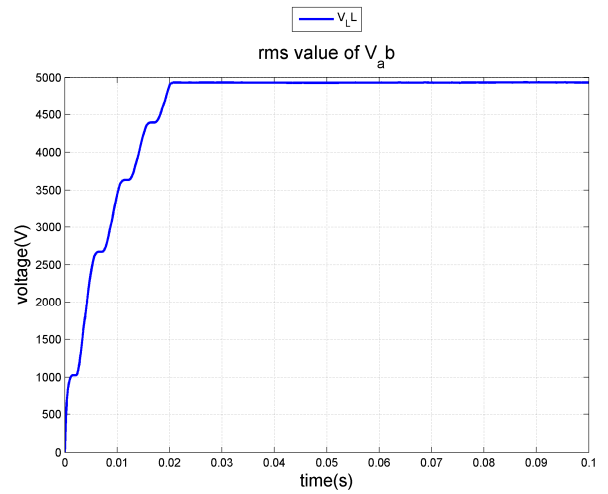
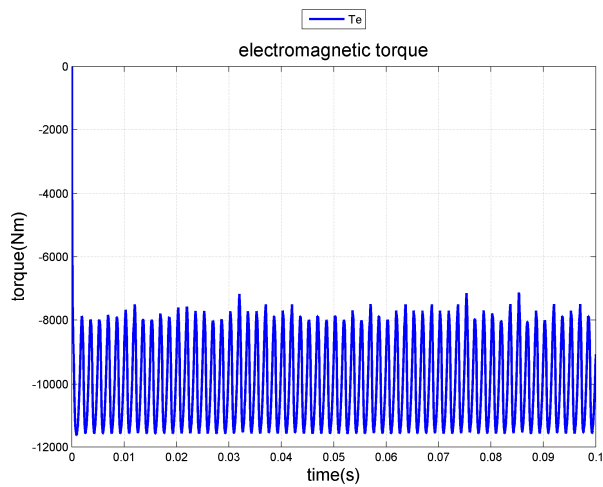


Figure 4.24 and 4.25:  $T_e$  and rms value of  $U_{LL}$  at  $\omega_s = 10$  m/s.

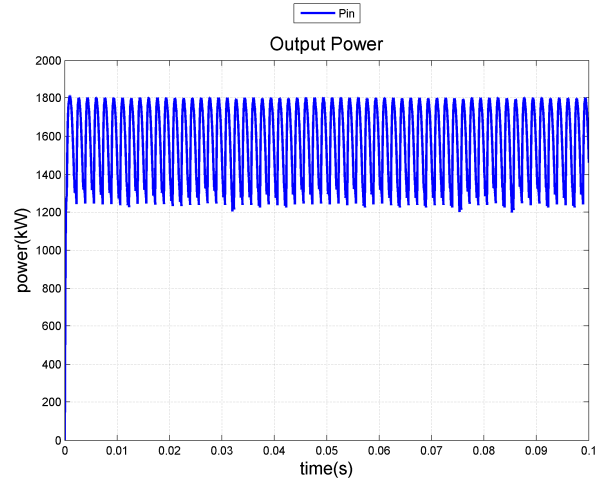
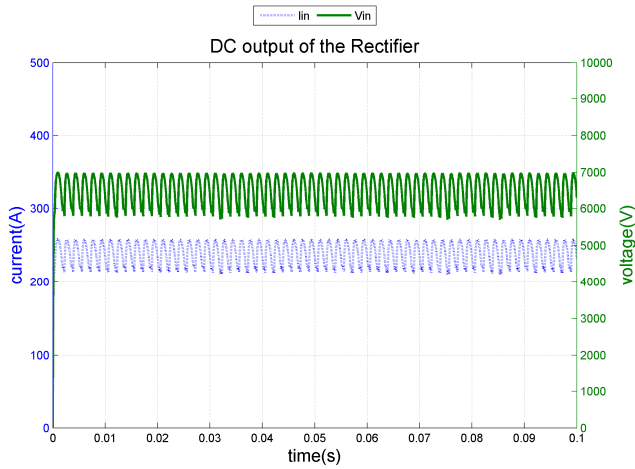


Figure 4.26 and 4.27: rectifier output voltage, current and power at  $\omega_s = 10$  m/s.

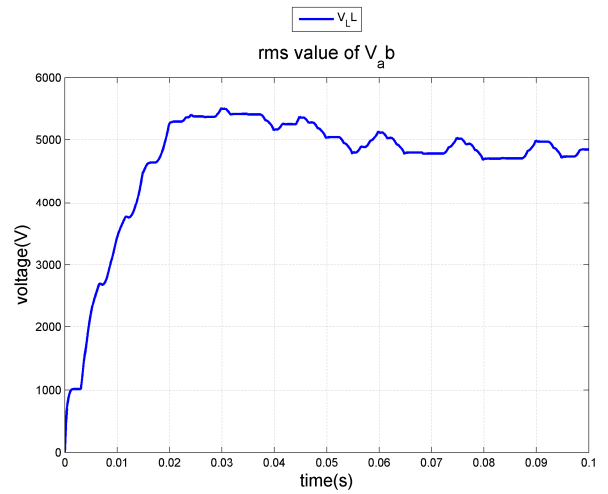
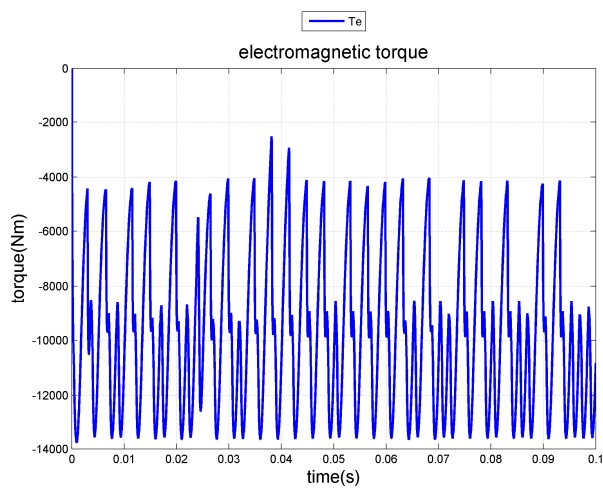


Figure 4.28 and 4.29:  $T_e$  and rms value of  $U_{LL}$  at  $\omega_s = 12$  m/s.

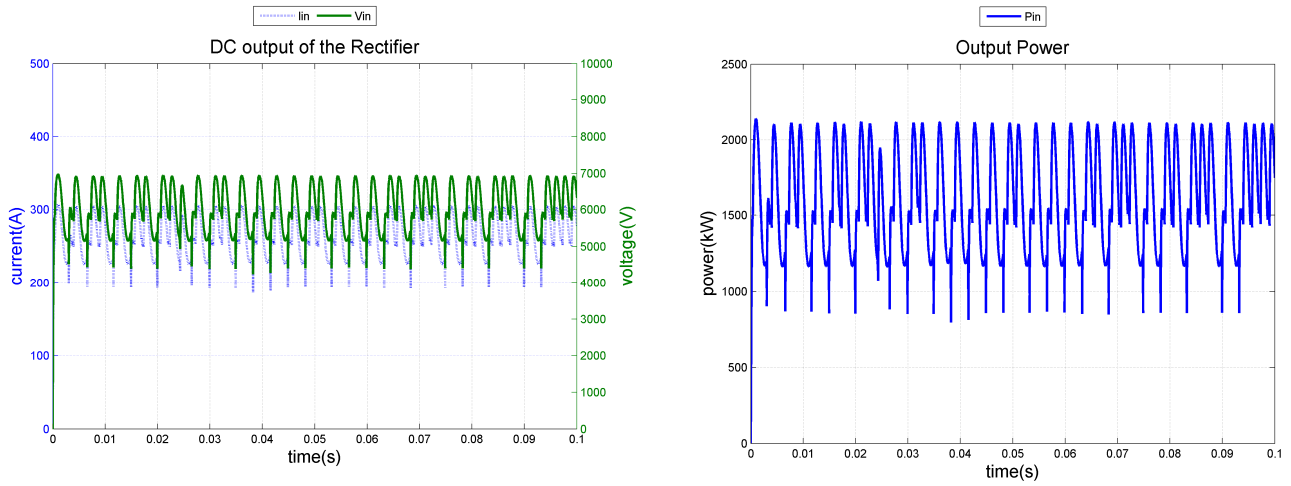


Figure 4.30 and 4.31: rectifier output voltage, current and power at  $\omega_s = 12$  m/s.

In the last figures, the ones corresponding to the rated operating point, it can be seen that the signals have peaks and large ripple. The problem could probably come from the generator block because the electromagnetic torque signal given has large oscillations. Also, the rms value of the generator output line-to-line voltage is not behaving as well as the other points. These strange results were only found at rated points.

### 4.4 Design of the boost converter

In Figure 4.32 the topology of the Simulink file with the whole system implemented is shown.

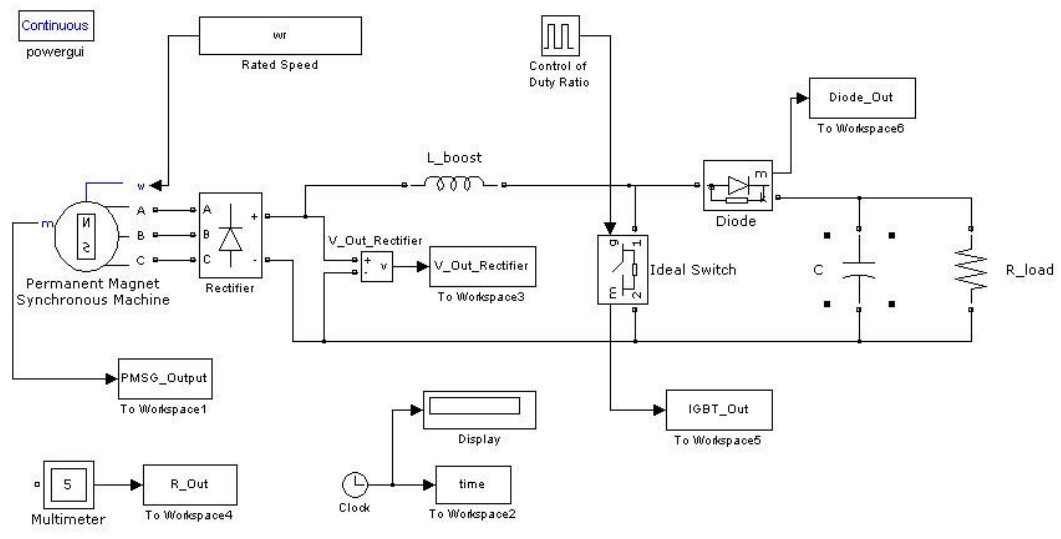


Figure 4.32: Simulink file of the whole system.

The equations used for the design of the step-up converter were shown and explained in Section 3.5 of Chapter 3. To calculate the different values of the Duty ratio, the maximum output voltage value expected,  $U_o = 6750$  V, and the line-to-line voltages of the generator in each operation point were used. The design steps given in [23] were followed.

$$D = 1 - \frac{U_{d,\min}}{U_o} \quad (4.4)$$

The values of  $D$  are listed on Table 4.4.

Table 4.4 Data used to calculate  $D$

Wind speed $\omega_s$ [m/s]	Rotor Speed $n_r$ [rpm]	Electric power $P_e$ [kW]	$U_{LL}$ [V]	$U_d$ [V]	Duty ratio ( $D$ )
4	8.7	100	2935	3962.3	0.413
5	9.6	225	3230	4360.5	0.354
6	11.4	350	3840	5184	0.232
8	14.6	800	4900	6615	0.02
10	14.8	1650	4950	6682.5	0.01
12	14.8	2000	5000	6750	0

The value of the Boost converter's inductance will change depending on the voltage levels, the switching frequency and the inductor current ripple at the different operating points. In each wind speed point, it can be calculated with the following equation [23]:

$$L_{boost} = \frac{U_d(U_o - U_{in})}{\Delta I_L f_s U_o} \quad (4.5)$$

Note that the higher the inductance is, the higher the maximum output current is but, on the other hand, the higher the size is. The inductor current ripple can be estimated with [23]:

$$\Delta I_L = (0.2 \leftrightarrow 0.4) \cdot I_{o,\max} \frac{U_o}{U_d} \quad (4.6)$$



Table 4.5 Ideal values of inductance, ripple current (30% chosen) and duty ratio

Wind speed $\omega_s$ [m/s]	Electric power $P_e$ [kW]	$U_d$ [V]	Duty ratio ( $D$ )	$L_{boost}$ [mH] (ideal)	$\Delta I_L$ [A]
4	100	3962.3	0.413	216.1	7.5714
5	225	4360.5	0.354	99.7	15.4799
6	350	5184	0.232	59.4	20.2546
8	800	6615	0.02	3.6	36.2812
10	1650	6682.5	0.01	0.90214	74.0741
12	2000	6750	0	0	88.8889

It is necessary to calculate the value of the output capacitor to minimize the ripple on the output voltage. To adjust the capacitance for a desired output voltage ripple from [23] it can be used:

$$C_{out(min)} = \frac{I_{o,max} \cdot D}{f_s \cdot \Delta U_o} \quad (4.7)$$

In the simulations a desired output voltage ripple of 10% was considered. As it is said in paper [23], any capacitor value above the recommended minimum can be used if the converter has an external compensation. In this thesis a value of  $C_{out} = 100 \mu\text{F}$  was used, because it gives better response of the output voltage. The minimum output capacitance values are shown in Table 4.6.

Table 4.6 Minimum output capacitance values

Wind speed $\omega_s$ [m/s]	Electric power $P_e$ [kW]	$U_d$ [V]	Duty ratio ( $D$ )	$C_{out(min)}$ [ $\mu\text{F}$ ]
4	100	3962.3	0.413	11.641
5	225	4360.5	0.354	23.862
6	350	5184	0.232	29.621
8	800	6615	0.02	37.926
10	1650	6682.5	0.01	75.325
12	2000	6750	0	87.791

Once all the values are calculated and defined, to start the simulations it is necessary to select a converter's inductance value, a switching frequency and maybe increase a bit the duty cycle at low speeds in order to rise up the output voltage and the power levels.

## 4.5 Simulation of the boost converter

In the next figures some of the main important graphics resulted from the simulations are shown. The parameters can be found in the previous tables and listed below:

- $L_{boost} = 10 \text{ mH}$  and  $C_{out} = 100 \text{ }\mu\text{F}$ .
- Switching frequency:  $f_s = 1000 \text{ Hz}$ .

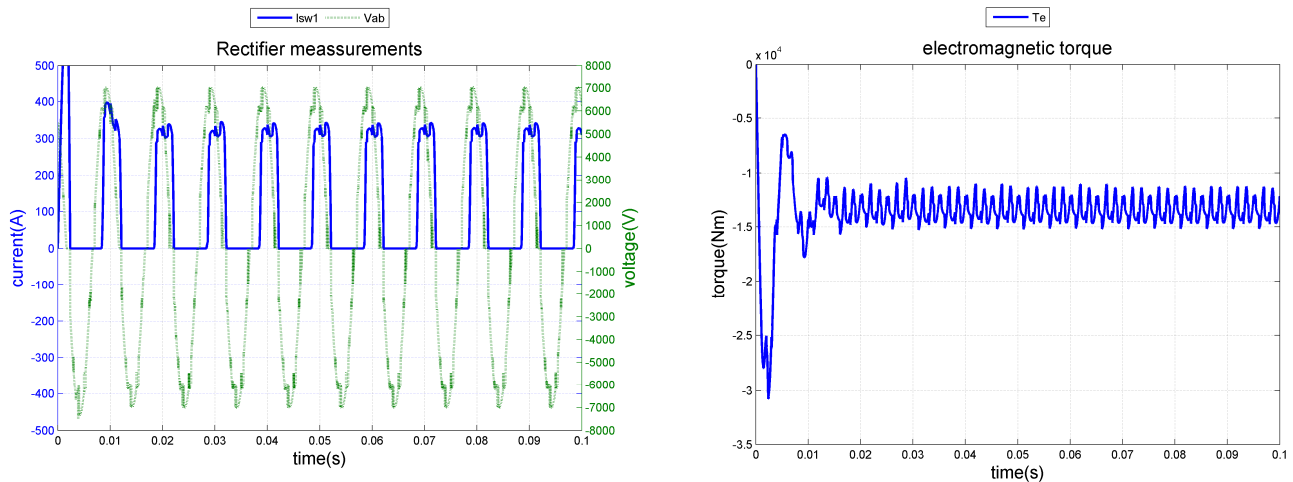


Figure 4.33 and 4.34: Rectifier measurements and  $T_e$  at  $\omega_s = 12 \text{ m/s}$ .

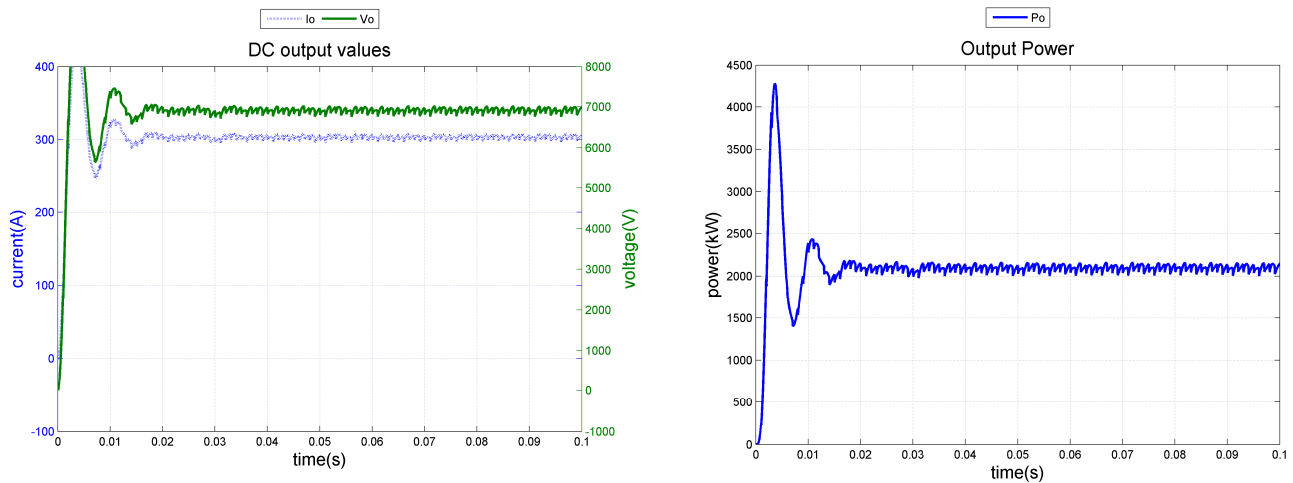


Figure 4.35 and 4.36: rectifier output voltage, current and power at  $\omega_s = 12 \text{ m/s}$ .

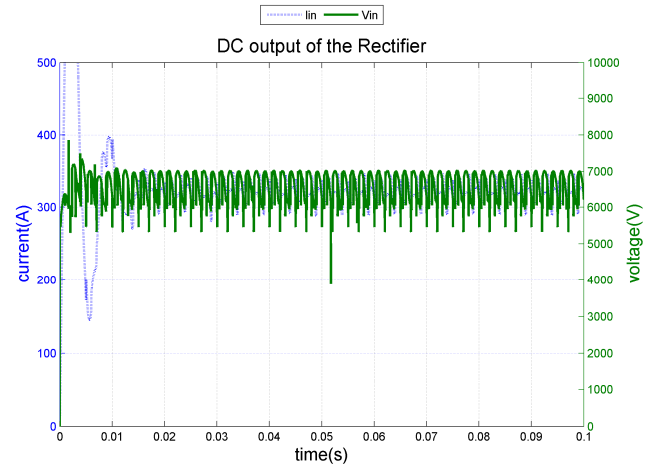
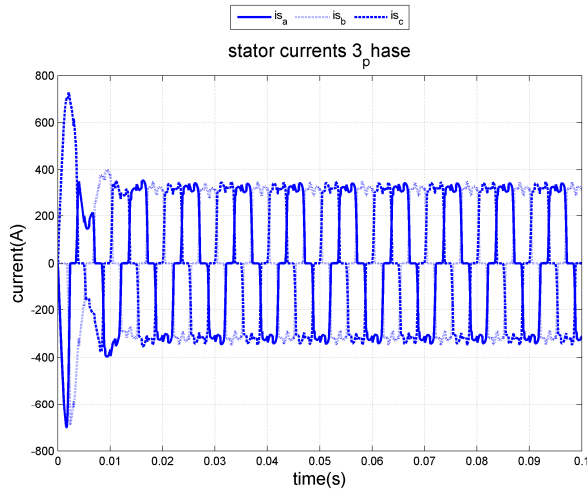


Figure 4.37 and 4.38: stator currents and DC rectifier output at  $\omega_s = 12$  m/s.

At rated values, the Boost converter is working as expected. It is providing at the DC output point, the rated voltage given at the output of the rectifier. The reason is that the step-up converter was designed to supply the rated voltage, 6750 V, at the output at every operating condition. When the wind speed is the nominal, 12 m/s, the converter duty ratio is small because is not necessary to increase the voltage level too much, only to compensate the possible losses of the different devices. In order to avoid conduction losses across the diode at this operating point, a switch in shunt with this device could be used to disconnect it. At the next operating point, wind speeds of 10 m/s the behavior is also pretty successful.

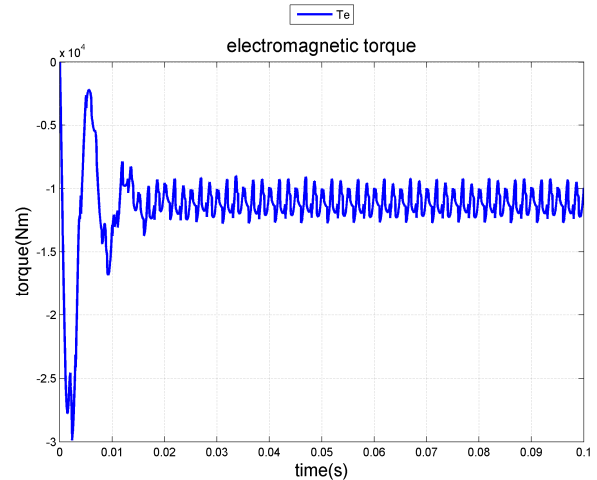
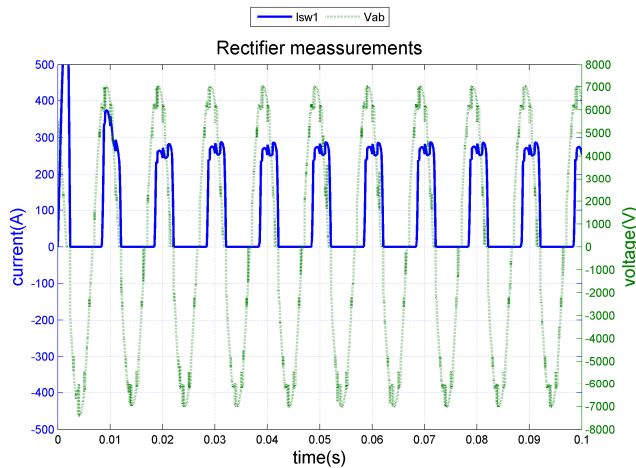


Figure 4.39 and 4.40: Rectifier measurements and  $T_e$  at  $\omega_s = 10$  m/s.

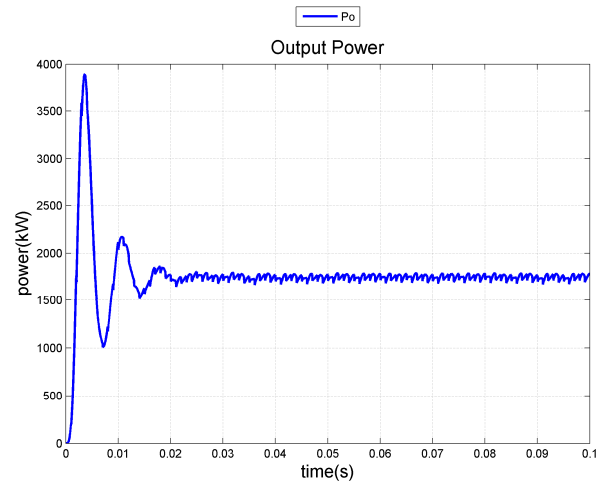
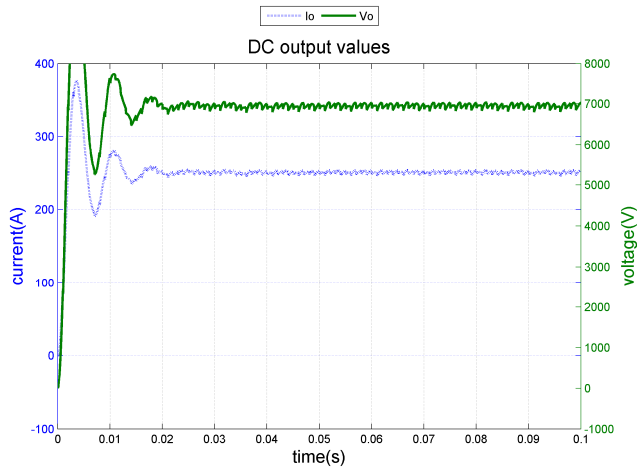


Figure 4.41 and 4.42: output voltage, current and power at  $\omega_s = 10$  m/s.

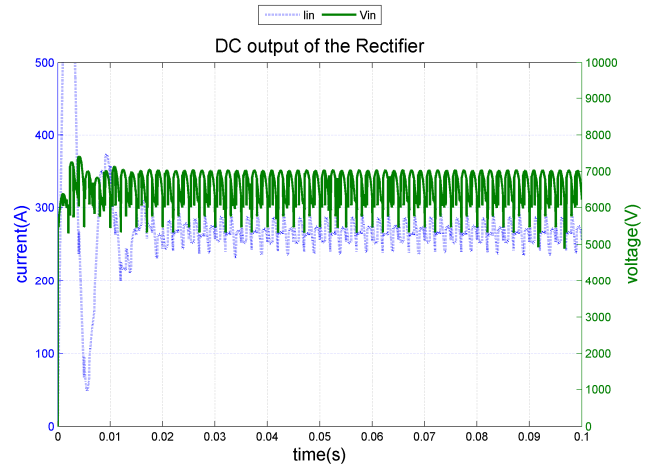
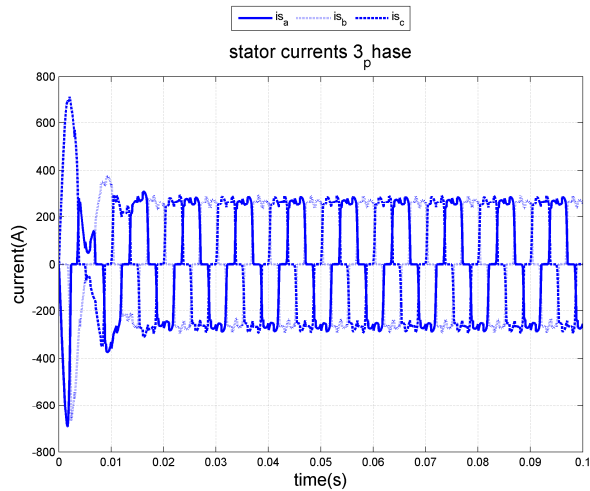


Figure 4.43 and 4.44: stator currents and DC rectifier output at  $\omega_s = 10$  m/s.

In the moment that the wind speed starts to decrease, the duty ratio is increasing because this device is trying to maintain the rated output voltage, and the difference between the input and the output voltages in the Boost converter is bigger. In the following figures, corresponding to the next operating point, it can be observed that the step-up converter continues to work correctly. 6750 V can be found at the output, and also the output power is 800 kW, the value expected at that wind speeds.

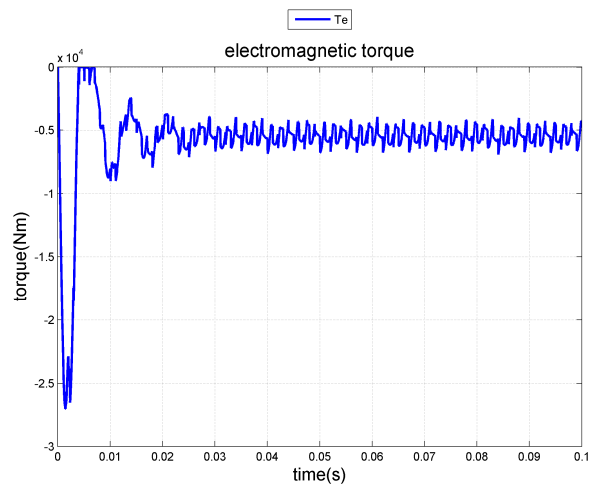
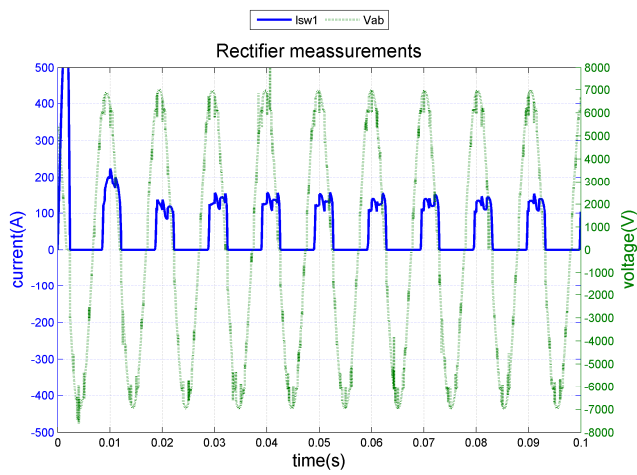


Figure 4.45 and 4.46: Rectifier measurements and  $T_e$  at  $\omega_s = 8$  m/s.

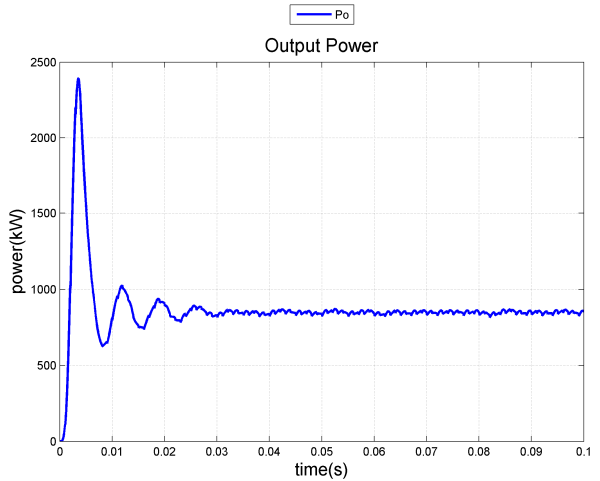
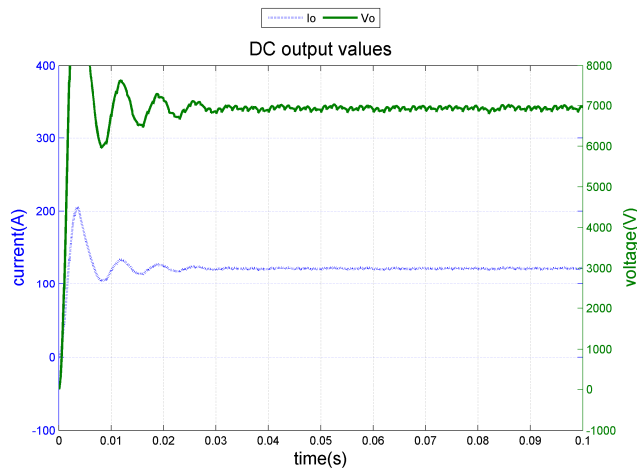


Figure 4.47 and 4.48: output voltage, current and power at  $\omega_s = 8$  m/s.

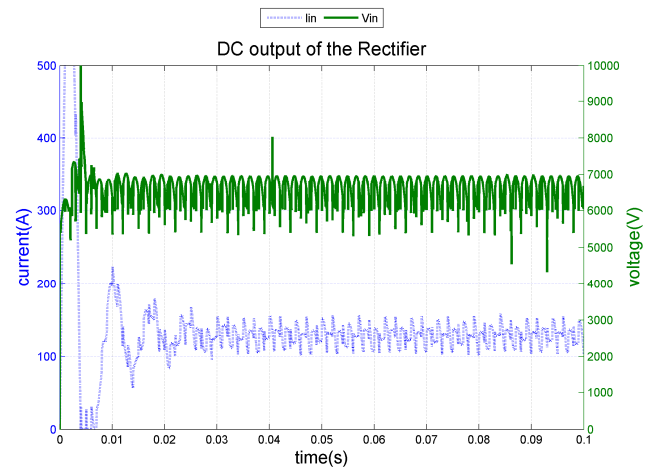
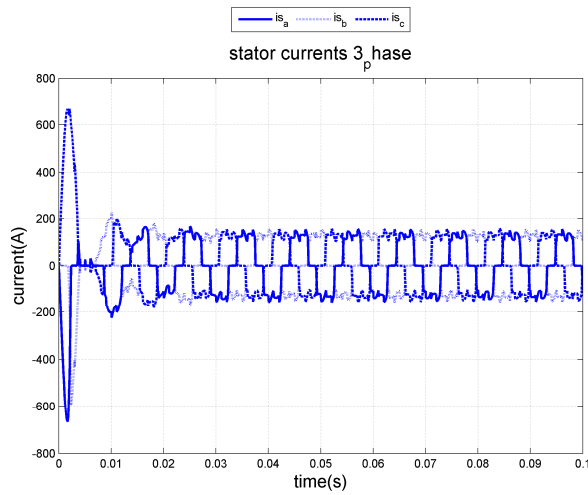


Figure 4.49 and 4.50: stator currents and DC rectifier output at  $\omega_s = 8$  m/s.

The results obtained show that at wind speeds close to the rated speed, the Boost converter could be an optimum solution to control the DC generated energy.

In the simulations, an ideal switch was used, but an IGBT can be considered. This device requires to be controlled. A suggestion is to use the current control system that was carried out in a previous Master Thesis [8]. In this project, a control of the current in the inductor of the step-up converter was done to control the torque of the generator and to protect the semiconductors in case of short-circuits.

At low speeds, it was found that the system does not behave properly. The output voltage and power values were not the expected ones. The design of the converter was made to have the rated voltage at the output of the system, as it can be observed in the figures shown before. But it has to be investigated in the future work, why at low speeds the simulations do not work.

## 5 Chapter Five

### Analytical studies

In this chapter the possible size of the Boost converter's inductor is calculated, considering the design values and the operating conditions. Also, a study of losses in some of the devices that are used in the system in order to have a better idea about the efficiency of the topology purposed is carried out.

#### 5.1 Design of the inductor

In this section, the size of the inductor used in the Boost converter is estimated. The dimensions can be seen in Figure 5.1.

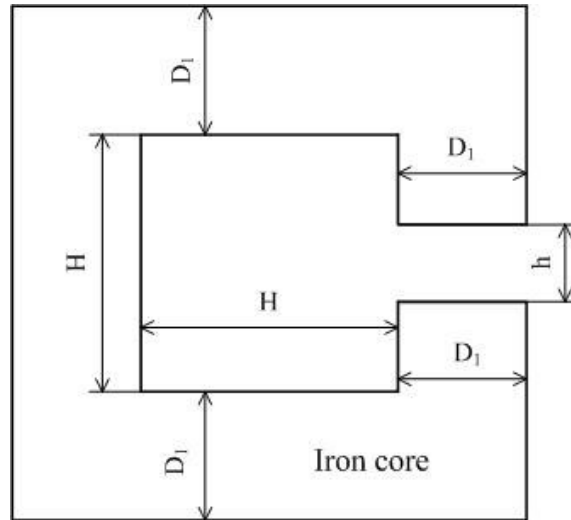


Figure 5.1: Dimensions of the inductor.

The average flux in the inductor is given by the following equation:

$$\psi_{av} = LI_{av} \quad (5.1)$$

Also it can be written that:

$$LI_{av} = NA_{core} B_{av} \quad (5.2)$$

At rated values, it is possible to say that the expected ripple could be 10% of the rated current, so in the flux density the ripple is the same.

The saturation flux density of the iron is 2.35 T, and for safety reasons an average value between 1.5 T and 2 T can be assumed.

Using (5.2) and giving several values to  $D_1$ , so  $A_{core}$  can be known, it is possible to compute the value of  $N$ . Considering the permeability of the iron infinite:

$$\frac{B_{av}}{\mu_0} h = NI_{av} \quad (5.3)$$

$$h = \frac{\mu_0 NI_{av}}{B_{av}} \quad (5.4)$$

Using VACOFLUX 48 as the material for the core, from the manufacturer's data sheets the following values useful for the estimated calculations can be considered [24]:

- Very low losses at flux densities between 1.8 T and 2.2 T.
- Density:  $\rho_{core} = 8.12 \text{ g/cm}^3$ .

The value of the inductance was considered in the previous chapter to be  $L = 10 \text{ mH}$ . In the data sheets of core material it is said that the lower losses are given at flux densities between 1.8 T and 2.2 T, so an average value of  $B_{av} = 1.5 \text{ T}$  and  $B_{av} = 2 \text{ T}$  was considered. The maximum current values that can be reached in the system are at rated operating points. This current level is  $I_{o,max} = I_{av} = 296 \text{ A}$ , that is the same that can pass through the inductor. Then, it is possible to calculate the relation  $NA_{core}$  with (5.2). The length of the air gap can be estimated with (5.4), and with the following expression the iron volume is

$$V_{core} = D^2(4(H + D) - h) \quad (5.5)$$

Knowing the iron density given above, the weight of the iron can be calculated, and then, an idea of the possible size of the inductor. In Table 5.1 the different values are listed.

*Table 5.1 Design of the inductor values*

$B_{av}$ [T]	$N \cdot A_{core}$ [turns m <sup>2</sup> ]	$N$ [turns]	$D_1$ [cm]
1.5	1.9733	10	44,42
2	1.48	10	38.47

To estimate a value of the core section, the maximum current in the inductor is used,  $I_{o,max} = I_{av} = 296$ , and the density current admitted that is  $4 \text{ A/mm}^2$ . Then, the section of the cable is  $74 \text{ mm}^2$ , so the diameter is approximately 10 mm.



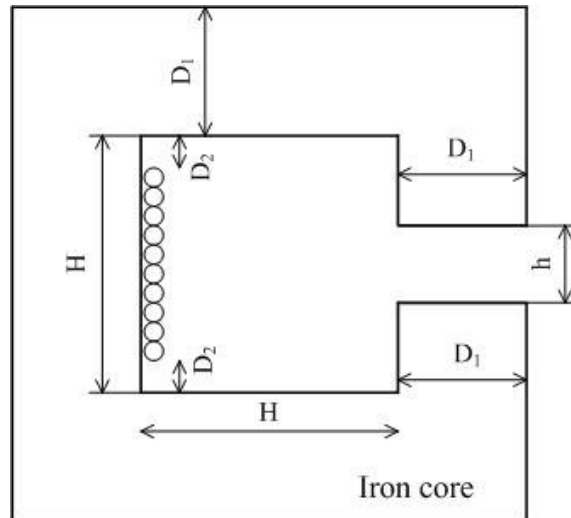


Figure 5.2: Dimensions of the inductor and cable.

In Figure 5.2 the cable with its turns was added. Due to the small expected cable section, 10 turns was considered to be an optimum estimated value. With the diameter of the cable and the space left between the extreme cables and the iron core the value of  $H$  can be calculated:  $H = 14$  cm.

Finally, the size of the inductor is presented in Table 5.2, calculating the mass with (5.6).

$$\rho_{core} = \frac{mass}{V} \quad (5.6)$$

Table 5.2 Size values of the inductor

$B_{av}$ [T]	$D_1$ [cm]	$h$ [cm]	$V$ [cm <sup>3</sup> ]	mass [kg]
1.5	44,42	0.25	460590	3740
2	38.47	0.19	460710	3741

## 5.2 Calculation of losses

The efficiency of a system can be estimated considering its losses. A system is more efficient if it has fewer losses.

In this case, some studies to calculate the losses through the diode rectifier, the switch, the inductor and the diode of the converter are presented. The results are listed in Table 5.3 as a percentage of the total generated power for the different wind speeds.

First of all, the losses through the diode rectifier are calculated. Considering a safety margin of 50% for the voltage, the number of diodes in series necessary can be obtain from:

$$n_{series} = 1.5 \frac{U_d}{V_{RRM}} \quad (5.7)$$

In the diode rectifier used in this work, the output rated voltage is  $U_d = 6750$  V, so the number of diodes necessary are:

$$n_{series} = 1.5 \frac{6750}{4500} = 2.25 \approx 2 \text{ diodes.}$$

Then, the conduction losses in the rectifier can be quantified using (5.8):

$$P_{cond,rect} = 2n_s I_d V_{on,diode} \quad (5.8)$$

Now, the following equations can be used to calculate the switching and conduction losses in the switch, IGBT [8]:

$$P_{switch,IGBT} = V_{IGBT} I_d \frac{t_r + t_f}{2K} f_s \quad (5.9)$$

$$P_{cond,IGBT} = n_{series,IGBT} V_{IGBT} I_{d,av} \quad (5.10)$$

The losses in the diode of the boost converter are computed with the same equation used for the IGBT, (5.10). In the diode  $I_{d,av} = (1-D)I_d$ , and in the IGBT is  $I_{d,av} = DI_d$ .

The losses in the inductor are the core losses and the copper losses:

$$P_{copper} = R_L I_d^2 \quad (5.11)$$

$$R_L = \rho_L \frac{length}{Area} = \rho_L \frac{H}{D_1^2} \quad (5.12)$$

From the data sheet, with  $f_s = 1000$  Hz, the core losses of the inductor can be obtained. Also,  $\rho_L = 0.44 \text{ } \Omega\text{mm}^2/\text{m}$ .

Table 5.3 Losses in the components

Wind speed $\omega_s$ [m/s]	$P_{cond,rect}$ [%]	$P_{switch,IGBT}$ [%]	$P_{cond,IGBT}$ [%]	$P_{inductor}$ [%]	$P_{diode}$ [%]
8	0.2015	0.0013	0.0316	1.0288	0.0395
10	0.1954	6.1636e-004	0.0295	0.4988	0.0387
12	0.1922	5.0850e-004	0.0279	0.4115	0.0384

It can be observed that the losses in the components of the system are low compared with the total generated energy. The main losses occurred in the inductor, increasing when the wind speeds decrease. This is normal if it is considered that at low speeds, the generated power is less than the power at high speeds.

## 6 Chapter Six

### Conclusions

The use of SimPowerSystems is useful in order to be able to implement pretty fast electric power simulations. As it can be observed in Chapter 4, the Boost converter results to be a good option, at high wind speeds, to have a control on the DC rectified voltage and current.

The losses found in the system are considered to be acceptable for the power values considered. In the estimation of the inductor's size, it was found that this device is large. This could lead to high costs of manufacturing and maintenance.

It cannot be concluded if the system studied in this thesis is suitable or not to use at low wind speeds because there are not enough information. At low wind speeds some problems were found, but it could be for different reasons. One could be that SimPowerSystems is not a valid tool in these conditions. MATLAB define the blocks used in this software and the equations are given in the manual, but it is not perfectly known what is progressing inside the blocks. Another one could be that in MATLAB Simulink the dynamic response of the systems are simulated, and in case of desired steady state studies, it could be better to use other software more suitable for this purpose, or implement a control system.

#### 6.1 Future work

In this thesis, only the PMSG was simulated. Another option could be use an EMSG and compare the different results. A cost study of the system can be carried out to give a quantitative idea of the system.

In Section 4.5, a switch in shunt with the diode of the Boost converter was proposed in order to avoid conduction losses through the diode when the system is working at rated values. It can be investigated how to implement and control this switch, and how the use of this device affects the total losses.

An important challenge could be to investigate the problems found at low speeds. Blocks designed by the own user would give a better control on what is happening in the simulations, and then, maybe it could be possible to clarify the behavior of the system.

In order to have some control of the current and voltage that are flowing into the step-up converter, an IGBT rectifier can be implemented. Also, a complete dynamic performance to have a more realistic idea about the system proposed in this work is suggested.

Finally, it could be interesting to investigate a six-phase or nine-phase generator, and the possibility to install AC-side filters to remove the large ripple of the signals.

## 7 References

- [1] Andrew R. Henderson, Colin Morgan, Bernie Smith, Hans C. Sørensen, Rebecca J. Barthelmie, Bart Boesmans, “Offshore wind energy in Europe- A review of the state-of-the-art”, WIND ENERGY, Wind Energ. 2003; 6:35–52 (DOI: 10.1002/we.82). Review. Article.
- [2] Thomas Ackermann, “Wind power in power systems”, John Wiley & Sons, January 2005.
- [3] Stefan Lundberg, “Configuration study of large wind parks”, Thesis for the degree of Licentiate of Engineering, Department of Electric Power Engineering, CHALMERS UNIVERSITY OF TECHNOLOGY, Göteborg, Sweden, 2003.
- [4] J. F. Manwell, J. G. McGowan, A. L. Rogers, “Wind energy Explained: Theory, Design and Application”, John Wiley & Sons, Second Edition, 2009.
- [5] Juan M. Carrasco, Eduardo Galván, Ramón Portillo, “Wind turbine applications”, Department of Electronic Engineering, Engineering School, Seville University, Spain.
- [6] Elkinton, C. N. (2007) “Offshore Wind Farm Layout Optimization”, PhD dissertation, University of Massachusetts, Amherst.
- [7] Ned Mohan, Tore M. Undeland, William P. Robbins, “Power Electronics, Converters, Applications and Design”, John Wiley & Sons, Second Edition, 1995.
- [8] André Marques, “Design, Control, Simulation and Energy Evaluation of a DC Offshore Wind Park”, Master of Science Thesis, Department of Energy and Environment, Division of Electric Power Engineering, CHALMERS UNIVERSITY OF TECHNOLOGY, Göteborg, Sweden, 2009.
- [9] Ming Yin, Gengyin Li, Ming Zhou, Chengyong Zhao, “Modeling of the wind turbine with a permanent magnet synchronous generator for integration”, Power Engineering Society General Meeting, 2007. IEEE.
- [10] Hydro-Québec, “SimPowerSystems users’ guide”, Hydro-Québec and The Math Works, 1998-2010.
- [11] Torbjörn Thiringer, Julia Paixao, Massimo Bongiorno, ”Monitoring of the ride-through ability of a 2MW Wind turbine in Tvååker, Halland”, Elforsk rapport, February 2009.
- [12] Muhammad H. Rashid, Ph.D., Fellow IEE, Fellow IEEE , “Power Electronics Handbook, Devices, Circuits, and Applications”, Elsevier, Second Edition, 2007.
- [13] S. Jöckel, “Gearless wind energy converters with permanent magnet generators an option for the future?”, European Wind Conference 1996, Goteborg, Sweden.
- [14] Yashodhan Prakash Agalgaonkar, “Investigation of Generating Systems for DC connected Wind Turbine”, Master Thesis, Department of Energy and Environment, CHALMERS UNIVERSITY OF TECHNOLOGY, Göteborg, Sweden, 2006.

- [15] Torbjörn Thiringer, "Lecture slides from Power Electronic Devices and Applications course", Chalmers University of Technology, Department of Energy and Environment, Division of Electric Power Engineering.
- [16] B. Normark, E. Koldby Nielsen, "Advanced power electronics for cable connection of offshore wind," in Proc. Copenhagen Offshore Wind 05, 2005.
- [17] S. Meier, S. Norrga, H.-P. Nee, "New Voltage Source Converter Topology for HVDC Grid Connection of Offshore Wind Farms", Department of Electrical Engineering, Royal Institute of Technology, Stockholm, Sweden.
- [18] N. M. Kirby, Lie Xu, Martin Luckett, Werner Siepmann, "HVDC transmission for large offshore wind farms", Power Engineering Journal, June 2002.
- [19] Kjell Eriksson, Christer Liljegren, Kent Sobrink, "HVDC Light Experiences applicable for power transmission from offshore wind power parks", ABB Library.
- [20] Gunnar Asplund, "Sustainable energy systems with HVDC transmission", Power Engineering Society General Meeting, 2004, IEEE.
- [21] Lennart Harnefors, "Control of Variable-Speed Drives", Applied Signal Processing and Control, Department of Electronics, Mälardalen University, Västerås, Sweden, 2002
- [22] Ming Yin, Gengyin Li, Ming Zhou, Chengyong Zhao, "Modeling of the wind turbine with a permanent magnet synchronous generator for integration", Power Engineering Society General Meeting, 2007, IEEE.
- [23] Brigitte Hauke, "Basic Calculation of a Boost Converter's Power Stage", Low Power DC/DC Application, Application Report, Texas Instruments (www.ti.com), November 2009 - Revised July 2010.
- [24] Vacuumschmelze, "Soft Magnetic Cobalt-Iron-Alloys, VACOFLUX 48, VACOFLUX 50, VACODUR 50, VACOFLUX 17", Data sheets, Edition 2001, ([http://www.vacuumschmelze.de/fileadmin/documents/broschueren/agv/Pht-004\\_e.pdf](http://www.vacuumschmelze.de/fileadmin/documents/broschueren/agv/Pht-004_e.pdf)).
- [25] Thomas Setz, "Applying Fast Recovery Diodes", Diodes for IGCT- and GTO applications, ABB Switzerland Ltd, Semiconductors, December 2008.

## Appendix

### *MATLAB code used for the calculation of the generator output voltage values*

```
%*****  
%  
% RunFile_PMSG  
%  
% Sergio García Colino,  
% 01-10-2010  
%*****  
clear  
close all  
clc  
  
% VARIABLE DEFINITIONS  
P_rated=2e6;  
np=4;  
R_PMSG=0.1;  
L_PMSG_d=1.5e-3;  
L_PMSG_q=1.5e-3;  
Ud_rated=5000;  
f_rated=100;  
  
% SELECT THE CASE YOU WANT TO SIMULATE  
% case1=wind speed=4 m/s  
% case2=wind speed=5 m/s  
% case3=wind speed=6 m/s  
% case4=wind speed=8 m/s  
% case5=wind speed=10 m/s  
% case6=wind speed=12 m/s  
select_case='case1';  
  
switch lower(select_case)  
case 'case1'  
nr=881.7568; % wtr=8.7 %rpm;  
P=100e3; %W;  
R=86.3;  
case 'case2'  
nr=972.973; % wtr=9.6 %rpm;  
P=225e3; %W;  
R=46.55;  
case 'case3'  
nr=1155.4; % wtr=11.4 %rpm;  
P=350e3; %W;  
R=42.2;  
case 'case4'  
nr=1479.7; % wtr=14.6 %rpm;  
P=800e3; %W;  
R=30.2;  
case 'case5'  
nr=1500; % wtr=14.8 %rpm;  
P=1650e3; %W;  
R=15.4;  
case 'case6'  
nr=1500; % wtr=14.8 %rpm;  
P=2000e3; %W;  
R=12.25;
```

```

        otherwise
            disp('Wrong case selection---Case6(Rated values) was selected
by default')
            nr=1500;          % wtr=14.8 %rpm;
            P=2000e3;        %W;
            R=12.25;
        end

% ng=1500/14.8=101.3514; gearbox ratio
wr=nr*pi/30;
T=(P/wr)*1000

sim('PMSG')
whos

% DISTRIBUTING THE PMSG-PARAMETERS
is_a=PMSG_Output(:,1);
is_b=PMSG_Output(:,2);
is_c=PMSG_Output(:,3);
is_d=PMSG_Output(:,4);
is_q=PMSG_Output(:,5);
vs_d=PMSG_Output(:,6);
vs_q=PMSG_Output(:,7);
hall_a=PMSG_Output(:,8);
hall_b=PMSG_Output(:,9);
hall_c=PMSG_Output(:,10);
RotorSpeed=PMSG_Output(:,11);
RotorAngle=PMSG_Output(:,12);
Te=PMSG_Output(:,13);

% % MEASUREMENTS OF THE LINE-TO-LINE RMS VALUES OF VOLTAGE AND
CURRENT
I=I_rms;
V_line_rms=V_LL_rms;
V_line=V_LL;

% % MEASUREMENTS OF CURRENT AND VOLTAGE IN THE RESISTOR
I_R=R_Out(:,1);
V_R=R_Out(:,2);

% % PLOTTING THE VARIABLES

% Stator currents three-phase and d-q axes
figure(1);
plot(time,is_a,time,is_b,time,is_c,'LineWidth',2,'MarkerSize',3),grid
;
title('stator currents 3_phase');
xlabel('time(s)', 'fontsi', [13]);
ylabel('current(A)', 'fontsi', [13]);
legend('is_a', 'is_b', 'is_c', 'Location', 'NorthOutside', 'Orientation', '
horizontal');

%%_PRINT_%%_PRINT_%%_PRINT_%%_PRINT_%%_PRINT_%%_PRINT_%%_PRINT_%%_PRINT_%%_PRINT_%%_PRINT
direction=['C:\Dokument\MASTER THESIS\SIMULINK
FILES\PMSG\PMSG\figures\'];
name=[direction, 'stator currents 3_phase'];
print('-dpng', '-noui', '-r300', [name, '.png']);
%%_PRINT_%%_PRINT_%%_PRINT_%%_PRINT_%%_PRINT_%%_PRINT_%%_PRINT_%%_PRINT_%%_PRINT_%%_PRINT

```



```

figure(2);
plot(time,is_d,time,is_q,'LineWidth',2,'MarkerSize',3),grid;
title('stator currents d-q');
xlabel('time(s)','fontsi',[13]);
ylabel('current(A)','fontsi',[13]);
legend('is_d','is_q','Location','NorthOutside','Orientation','horizontal');

%%_PRINT_%%_PRINT_%%_PRINT_%%_PRINT_%%_PRINT_%%_PRINT_%%_PRINT_%%_PRINT
direction=['C:\Dokument\MASTER THESIS\SIMULINK
FILES\PMSG\PMSG\figures\'];
name=[direction,'stator currents d-q'];
print('-dpng','-noui','-r300',[name,'.png']);
%%_PRINT_%%_PRINT_%%_PRINT_%%_PRINT_%%_PRINT_%%_PRINT_%%_PRINT_%%_PRINT

% Stator voltages in d-q axes
figure(3);
plot(time,vs_d,time,vs_q,'LineWidth',2,'MarkerSize',3),grid;
title('stator voltages d-q');
xlabel('time(s)','fontsi',[13]);
ylabel('voltage(V)','fontsi',[13]);
legend('vs_d','vs_q','Location','NorthOutside','Orientation','horizontal');

%%_PRINT_%%_PRINT_%%_PRINT_%%_PRINT_%%_PRINT_%%_PRINT_%%_PRINT_%%_PRINT
direction=['C:\Dokument\MASTER THESIS\SIMULINK
FILES\PMSG\PMSG\figures\'];
name=[direction,'stator voltages d-q'];
print('-dpng','-noui','-r300',[name,'.png']);
%%_PRINT_%%_PRINT_%%_PRINT_%%_PRINT_%%_PRINT_%%_PRINT_%%_PRINT_%%_PRINT

% Rotor speed
figure(4);
plot(time,RotorSpeed,'LineWidth',2,'MarkerSize',3),grid;
title('Rotor Speed');
xlabel('time(s)','fontsi',[13]);
ylabel('speed(rad/s)','fontsi',[13]);
legend('Rotorspeed','Location','NorthOutside','Orientation','horizontal');

%%_PRINT_%%_PRINT_%%_PRINT_%%_PRINT_%%_PRINT_%%_PRINT_%%_PRINT_%%_PRINT
direction=['C:\Dokument\MASTER THESIS\SIMULINK
FILES\PMSG\PMSG\figures\'];
name=[direction,'Rotor Speed'];
print('-dpng','-noui','-r300',[name,'.png']);
%%_PRINT_%%_PRINT_%%_PRINT_%%_PRINT_%%_PRINT_%%_PRINT_%%_PRINT_%%_PRINT

% Electromagnetic torque
figure(5);
plot(time,Te,'LineWidth',2,'MarkerSize',3),grid;
title('electromagnetic torque');
xlabel('time(s)','fontsi',[13]);
ylabel('torque(Nm)','fontsi',[13]);
legend('Te','Location','NorthOutside','Orientation','horizontal');

%%_PRINT_%%_PRINT_%%_PRINT_%%_PRINT_%%_PRINT_%%_PRINT_%%_PRINT_%%_PRINT

```

```

direction=['C:\Dokument\MASTER THESIS\SIMULINK
FILES\PMSG\PMSG\figures\'];
name=[direction,'electromagnetic torque'];
print('-dpng', '-noui', '-r300', [name,'.png']);
%%_PRINT_%%_PRINT_%%_PRINT_%%_PRINT_%%_PRINT_%%_PRINT_%%_PRINT_%%_PRINT

% rms voltage line-to-line
figure(6);
plot(time,V_line_rms,'LineWidth',2,'MarkerSize',3),grid;
title('rms V_ab');
xlabel('time(s)', 'fontsi', [13]);
ylabel('voltage(V)', 'fontsi', [13]);
legend('V_ab','Location','NorthOutside','Orientation','horizontal');

%%_PRINT_%%_PRINT_%%_PRINT_%%_PRINT_%%_PRINT_%%_PRINT_%%_PRINT_%%_PRINT
direction=['C:\Dokument\MASTER THESIS\SIMULINK
FILES\PMSG\PMSG\figures\'];
name=[direction,'rms V_ab'];
print('-dpng', '-noui', '-r300', [name,'.png']);
%%_PRINT_%%_PRINT_%%_PRINT_%%_PRINT_%%_PRINT_%%_PRINT_%%_PRINT_%%_PRINT

% AC output in the resistor
figure(7);
[AX,H1,H2] = plotyy(time,I_R,time,V_R),grid;
set(get(AX(1),'Ylabel'),'String','current(A)', 'fontsi', [13]);
set(get(AX(2),'Ylabel'),'String','voltage(V)', 'fontsi', [13]);
set(H2, 'LineWidth',2,'MarkerSize',3);
set(H1, 'LineWidth',2,'MarkerSize',3);
xlabel('time(s)', 'fontsi', [13]);
title('AC output in the resistor');
legend('I_R','V_R','Location','NorthOutside','Orientation','horizontal');

%%_PRINT_%%_PRINT_%%_PRINT_%%_PRINT_%%_PRINT_%%_PRINT_%%_PRINT_%%_PRINT
direction=['C:\Dokument\MASTER THESIS\SIMULINK
FILES\PMSG\PMSG\figures\'];
name=[direction,'AC output in the resistor'];
print('-dpng', '-noui', '-r300', [name,'.png']);
%%_PRINT_%%_PRINT_%%_PRINT_%%_PRINT_%%_PRINT_%%_PRINT_%%_PRINT_%%_PRINT

% Output power in AC
P=sqrt(3)*I.*V_line_rms;

figure(8);
plot(time,P/1000,'LineWidth',2,'MarkerSize',3),grid;
title('Output Power');
xlabel('time(s)', 'fontsi', [13]);
ylabel('power(kW)', 'fontsi', [13]);
legend('P','Location','NorthOutside','Orientation','horizontal');

%%_PRINT_%%_PRINT_%%_PRINT_%%_PRINT_%%_PRINT_%%_PRINT_%%_PRINT_%%_PRINT
direction=['C:\Dokument\MASTER THESIS\SIMULINK
FILES\PMSG\PMSG\figures\'];
name=[direction,'Output Power'];
print('-dpng', '-noui', '-r300', [name,'.png']);
%%_PRINT_%%_PRINT_%%_PRINT_%%_PRINT_%%_PRINT_%%_PRINT_%%_PRINT_%%_PRINT

```

```

% line-to-line PMSG output voltage
figure(9);
plot(time,V_line,'LineWidth',2,'MarkerSize',3),grid;
title('V_ab');
xlabel('time(s)','fontsi',[13]);
ylabel('voltage(V)','fontsi',[13]);
legend('V_ab','Location','NorthOutside','Orientation','horizontal');

%%_PRINT_%%_PRINT_%%_PRINT_%%_PRINT_%%_PRINT_%%_PRINT_%%_PRINT_
direction=['C:\Dokument\MASTER THESIS\SIMULINK
FILES\PMSG\PMSG\figures\'];
name=[direction,'V_ab'];
print('-dpng','-noui','-r300',[name,'.png']);
%%_PRINT_%%_PRINT_%%_PRINT_%%_PRINT_%%_PRINT_%%_PRINT_%%_PRINT_

```

***MATLAB code used for checking the behaviour of the three-phase full bridge diode rectifier using the load resistance***

```

%*****
%
% RunFile_PMSG
%
% Sergio Garcia Colino,
% 01-10-2010
%*****
clear
close all
clc

% VARIABLE DEFINITIONS
P_rated=2e6;
np=4;
R_PMSG=0.1;
L_PMSG_d=1.5e-3;
L_PMSG_q=1.5e-3;
Ud_rated=5000;
f_rated=100;

% SELECT THE CASE YOU WANT TO SIMULATE
% case1=wind speed=4 m/s
% case2=wind speed=5 m/s
% case3=wind speed=6 m/s
% case4=wind speed=8 m/s
% case5=wind speed=10 m/s
% case6=wind speed=12 m/s
select_case='case6';

switch lower(select_case)
case 'case1'
nr=881.7568; % wtr=8.7 %rpm;
P=100e3; %W;
U=3962.3;
R=(U^2)/P
case 'case2'
nr=972.973; % wtr=9.6 %rpm;
P=225e3; %W;

```

```

        U=4360.5;
        R=(U^2)/P
    case 'case3'
        nr=1155.4;           % wtr=11.4 %rpm;
        P=350e3;           %W;
        U=5184;
        R=(U^2)/P
    case 'case4'
        nr=1479.7;         % wtr=14.6 %rpm;
        P=800e3;           %W;
        U=6615;
        R=(U^2)/P
    case 'case5'
        nr=1500;           % wtr=14.8 %rpm;
        P=1650e3;          %W;
        U=6682.5;
        R=(U^2)/P
    case 'case6'
        nr=1500;           % wtr=14.8 %rpm;
        P=2000e3;          %W;
        U=6750;
        R=(U^2)/P
    otherwise
        disp('Wrong case selection---Case6(Rated values) was selected
by default')
        nr=1500;           % wtr=14.8 %rpm;
        P=2000e3;          %W;
        U=6750;
        R=(U^2)/P
end

% ng=1500/14.8=101.3514; gearbox ratio
wr=nr*pi/30;
T=(P/wr)*1000

sim('PMSG_Rectifier')
whos

% DISTRIBUTING THE PMSG-PARAMETERS
is_a=PMSG_Output(:,1);
is_b=PMSG_Output(:,2);
is_c=PMSG_Output(:,3);
is_d=PMSG_Output(:,4);
is_q=PMSG_Output(:,5);
vs_d=PMSG_Output(:,6);
vs_q=PMSG_Output(:,7);
hall_a=PMSG_Output(:,8);
hall_b=PMSG_Output(:,9);
hall_c=PMSG_Output(:,10);
RotorSpeed=PMSG_Output(:,11);
RotorAngle=PMSG_Output(:,12);
Te=PMSG_Output(:,13);

% voltage and current of the DC outputs,
% rectifier and the DC link

Vin=V_in;
Iin=R_Out(:,1);

```

```

% measurements of the Rectifier

Isw1=R_Out(:,2);
Vab=R_Out(:,3);

% % PLOTTING THE VARIABLES

% Stator currents three-phase and d-q axes
figure(1);
plot(time,is_a,'-','LineWidth',2,'MarkerSize',3),grid;
hold on
plot(time,is_b,':','LineWidth',2,'MarkerSize',3),grid;
hold on
plot(time,is_c,'--','LineWidth',2,'MarkerSize',3),grid;
hold on
title('stator currents 3_phase','fontsi',[16]);
xlabel('time(s)','fontsi',[15]);
ylabel('current(A)','fontsi',[15]);
legend('is_a','is_b','is_c','Location','NorthOutside','Orientation','horizontal');

%%_PRINT_%_PRINT_%%_PRINT_%_PRINT_%%_PRINT_%_PRINT_%%_PRINT_
direction=['C:\Dokument\MASTER THESIS\SIMULINK
FILES\PMSG\PMSG+Rectifier\figures\'];
name=[direction,'stator currents 3_phase'];
print('-dpng','-noui','-r300',[name,'.png']);
%%_PRINT_%_PRINT_%%_PRINT_%_PRINT_%%_PRINT_%_PRINT_%%_PRINT_

figure(2);
plot(time,is_d,'-','LineWidth',2,'MarkerSize',3),grid;
hold on
plot(time,is_q,':','LineWidth',2,'MarkerSize',3),grid;
hold on
title('stator currents d-q','fontsi',[16]);
xlabel('time(s)','fontsi',[15]);
ylabel('current(A)','fontsi',[15]);
legend('is_d','is_q','Location','NorthOutside','Orientation','horizontal');

%%_PRINT_%_PRINT_%%_PRINT_%_PRINT_%%_PRINT_%_PRINT_%%_PRINT_
direction=['C:\Dokument\MASTER THESIS\SIMULINK
FILES\PMSG\PMSG+Rectifier\figures\'];
name=[direction,'stator currents d-q'];
print('-dpng','-noui','-r300',[name,'.png']);
%%_PRINT_%_PRINT_%%_PRINT_%_PRINT_%%_PRINT_%_PRINT_%%_PRINT_

% Stator voltages in d-q axes
figure(3);
plot(time,vs_d,'-','LineWidth',2,'MarkerSize',3),grid;
hold on
plot(time,vs_q,':','LineWidth',2,'MarkerSize',3),grid;
hold on
title('stator voltages d-q','fontsi',[16]);
xlabel('time(s)','fontsi',[15]);
ylabel('voltage(V)','fontsi',[15]);
legend('vs_d','vs_q','Location','NorthOutside','Orientation','horizontal');

%%_PRINT_%_PRINT_%%_PRINT_%_PRINT_%%_PRINT_%_PRINT_%%_PRINT_

```

```

    direction=['C:\Dokument\MASTER THESIS\SIMULINK
FILES\PMMSG\PMMSG+Rectifier\figures\'];
    name=[direction,'stator voltages d-q'];
    print('-dpng', '-nou', '-r300', [name,'.png']);
%%_PRINT_%%_PRINT_%%_PRINT_%%_PRINT_%%_PRINT_%%_PRINT_%%_PRINT_%%_PRINT

% Rotor speed
figure(4);
plot(time,RotorSpeed,'LineWidth',2,'MarkerSize',3),grid;
title('Rotor Speed','fontsi',[16]);
xlabel('time(s)','fontsi',[15]);
ylabel('speed(rad/s)','fontsi',[15]);
legend('Rotorspeed','Location','NorthOutside','Orientation','horizontal');

%%_PRINT_%%_PRINT_%%_PRINT_%%_PRINT_%%_PRINT_%%_PRINT_%%_PRINT_%%_PRINT
    direction=['C:\Dokument\MASTER THESIS\SIMULINK
FILES\PMMSG\PMMSG+Rectifier\figures\'];
    name=[direction,'Rotor Speed'];
    print('-dpng', '-nou', '-r300', [name,'.png']);
%%_PRINT_%%_PRINT_%%_PRINT_%%_PRINT_%%_PRINT_%%_PRINT_%%_PRINT_%%_PRINT

% Electromagnetic torque
figure(5);
plot(time,Te,'LineWidth',2,'MarkerSize',3),grid;
title('electromagnetic torque','fontsi',[16]);
xlabel('time(s)','fontsi',[15]);
ylabel('torque(Nm)','fontsi',[15]);
legend('Te','Location','NorthOutside','Orientation','horizontal');

%%_PRINT_%%_PRINT_%%_PRINT_%%_PRINT_%%_PRINT_%%_PRINT_%%_PRINT_%%_PRINT
    direction=['C:\Dokument\MASTER THESIS\SIMULINK
FILES\PMMSG\PMMSG+Rectifier\figures\'];
    name=[direction,'electromagnetic torque'];
    print('-dpng', '-nou', '-r300', [name,'.png']);
%%_PRINT_%%_PRINT_%%_PRINT_%%_PRINT_%%_PRINT_%%_PRINT_%%_PRINT_%%_PRINT

% DC output of the Rectifier
figure(6);
[AX,H1,H2] = plotyy(time,Iin,time,Vin),grid;
set(AX(2),'Ylim',[0 10000]);
set(AX(2),'YTick',[0:1000:10000]);
set(AX(1),'Ylim',[0 500]);
set(AX(1),'YTick',[0:100:500]);
set(get(AX(1),'Ylabel'),'String','current(A)','fontsi',[15]);
set(get(AX(2),'Ylabel'),'String','voltage(V)','fontsi',[15]);
set(H2,'Line','-','LineWidth',2,'MarkerSize',3);
set(H1,'Line',':','LineWidth',2,'MarkerSize',3);
xlabel('time(s)','fontsi',[15]);
title('DC output of the Rectifier','fontsi',[16]);
legend('Iin','Vin','Location','NorthOutside','Orientation','horizontal');

%%_PRINT_%%_PRINT_%%_PRINT_%%_PRINT_%%_PRINT_%%_PRINT_%%_PRINT_%%_PRINT
    direction=['C:\Dokument\MASTER THESIS\SIMULINK
FILES\PMMSG\PMMSG+Rectifier\figures\'];
    name=[direction,'DC output of the Rectifier'];

```



```

    name=[direction,'rms value of V_ab'];
    print('-dpng', '-noui', '-r300', [name,'.png']);
%%_PRINT_%%_PRINT_%%_PRINT_%%_PRINT_%%_PRINT_%%_PRINT_%%_PRINT

```

### ***MATLAB code used for checking the behaviour of the three-phase full bridge diode rectifier using the DC-voltage source***

```

%*****
%
% RunFile_PMSG_Rectifier_DCsource
%
% Sergio García Colino,
% 01-10-2010
%*****

clear
close all
clc

% variable definitions

P_rated=2e6;
np=4;
R_PMSG=0.1;
L_PMSG_d=1.5e-3;
L_PMSG_q=1.5e-3;
Ud_rated=5000;
f_rated=100;

% Select the case you want to simulate
% case1=wind speed=4 m/s
% case2=wind speed=5 m/s
% case3=wind speed=6 m/s
% case4=wind speed=8 m/s
% case5=wind speed=10 m/s
% case6=wind speed=12 m/s
select_case='case6';

switch lower(select_case)
    case 'case1'
        nr=881.7568;    % wtr=8.7 %rpm;
        P=100e3;       %W;
        R=1;
        U_Rated=3710;
    case 'case2'
        nr=972.973;    % wtr=9.6 %rpm;
        P=225e3;       %W;
        R=1;
        U_Rated=4110;
    case 'case3'
        nr=1155.4;     % wtr=11.4 %rpm;
        P=350e3;       %W;
        R=1;
        U_Rated=4930;
    case 'case4'
        nr=1479.7;     % wtr=14.6 %rpm;
        P=800e3;       %W;
        R=1;

```



```

        U_Rated=6375;
    case 'case5'
        nr=1500;           % wtr=14.8 %rpm;
        P=1650e3;         %W;
        R=1;
        U_Rated=6430;
    case 'case6'
        nr=1500;           % wtr=14.8 %rpm;
        P=2000e3;         %W;
        R=1;
        U_Rated=6500;
    otherwise
        disp('Wrong case selection---Case6(Rated values) was selected
by default')
        nr=1500;           % wtr=14.8 %rpm;
        P=2000e3;         %W;
        R=1;
        U_Rated=6500;
end

% ng=1500/14.8=101.3514; gearbox ratio
wr=nr*pi/30;
T=(P/wr)

sim('PMSG_Rectifier_DCsource')
whos

% distributing the PMSG-parameters
is_a=PMSG_Output(:,1);
is_b=PMSG_Output(:,2);
is_c=PMSG_Output(:,3);
is_d=PMSG_Output(:,4);
is_q=PMSG_Output(:,5);
vs_d=PMSG_Output(:,6);
vs_q=PMSG_Output(:,7);
hall_a=PMSG_Output(:,8);
hall_b=PMSG_Output(:,9);
hall_c=PMSG_Output(:,10);
RotorSpeed=PMSG_Output(:,11);
RotorAngle=PMSG_Output(:,12);
Te=PMSG_Output(:,13);

% voltage and current of the DC outputs,
% rectifier and the DC link
Vin=V_in;
Iin=R_Out(:,1);

% measurements of the Rectifier
Isw1=R_Out(:,2);
Vab=R_Out(:,3);

% % PLOTTING THE VARIABLES

% Stator currents three-phase and d-q axes
figure(1);
plot(time,is_a,'-','LineWidth',2,'MarkerSize',3),grid;
hold on
plot(time,is_b,':','LineWidth',2,'MarkerSize',3),grid;

```





```

legend('Pin','Location','NorthOutside','Orientation','horizontal');

%%_PRINT_%%_PRINT_%%_PRINT_%%_PRINT_%%_PRINT_%%_PRINT_%%_PRINT_%%_PRINT_%%_PRINT_%%_PRINT
direction=['C:\Dokument\MASTER THESIS\SIMULINK
FILES\PMSG\PMSG+Rectifier+DCsource\figures\'];
name=[direction,'Output Power'];
print('-dpng','-noui','-r300',[name,'.png']);
%%_PRINT_%%_PRINT_%%_PRINT_%%_PRINT_%%_PRINT_%%_PRINT_%%_PRINT_%%_PRINT_%%_PRINT_%%_PRINT

% Rectifier measurements
figure(8);
[AX,H1,H2] = plotyy(time,Isw1,time,Vab),grid;
set(AX(2),'Ylim',[-8000 8000]);
set(AX(2),'YTick',[-8000:1000:8000])
set(AX(1),'Ylim',[-500 500]);
set(AX(1),'YTick',[-500:100:500]);
set(get(AX(1),'Ylabel'),'String','current(A)','fontsi',[15]);
set(get(AX(2),'Ylabel'),'String','voltage(V)','fontsi',[15]);
set(H1,'Line','-','LineWidth',2,'MarkerSize',3);
set(H2,'Line',':','LineWidth',2,'MarkerSize',3);
xlabel('time(s)','fontsi',[15]);
title('Rectifier measurements','fontsi',[16]);
legend('Isw1','Vab','Location','NorthOutside','Orientation','horizontal');

%%_PRINT_%%_PRINT_%%_PRINT_%%_PRINT_%%_PRINT_%%_PRINT_%%_PRINT_%%_PRINT_%%_PRINT_%%_PRINT
direction=['C:\Dokument\MASTER THESIS\SIMULINK
FILES\PMSG\PMSG+Rectifier+DCsource\figures\'];
name=[direction,'Rectifier meassurements'];
print('-dpng','-noui','-r300',[name,'.png']);
%%_PRINT_%%_PRINT_%%_PRINT_%%_PRINT_%%_PRINT_%%_PRINT_%%_PRINT_%%_PRINT_%%_PRINT_%%_PRINT

% rms value of the line-to-line PMSG output voltage

figure(9);
plot(time,V_ab_rms,'LineWidth',2,'MarkerSize',3),grid;
title('rms value of V_ab','fontsi',[16]);
xlabel('time(s)','fontsi',[15]);
ylabel('voltage(V)','fontsi',[15]);
legend('V_LL','Location','NorthOutside','Orientation','horizontal');

%%_PRINT_%%_PRINT_%%_PRINT_%%_PRINT_%%_PRINT_%%_PRINT_%%_PRINT_%%_PRINT_%%_PRINT_%%_PRINT
direction=['C:\Dokument\MASTER THESIS\SIMULINK
FILES\PMSG\PMSG+Rectifier+DCsource\figures\'];
name=[direction,'rms value of V_ab'];
print('-dpng','-noui','-r300',[name,'.png']);
%%_PRINT_%%_PRINT_%%_PRINT_%%_PRINT_%%_PRINT_%%_PRINT_%%_PRINT_%%_PRINT_%%_PRINT_%%_PRINT

```

### ***MATLAB code used for whole system, with the Boost converter***

```

%*****
%
% RunFile_PMSM_Rectifier_Ld_Boost
%
% Sergio García Colino,
% 01-10-2010
%*****

```

```

clear
close all
clc

% Variable definitions
P_rated=2e6;
np=4;
R_PMSG=0.1;
L_PMSG_d=1.5e-3;
L_PMSG_q=1.5e-3;
Ud_rated=5000;
f_rated=100;

% Desirable output voltage
Uo=6750;

% Select the case you want to simulate

% case1=wind speed=4 m/s
% case2=wind speed=5 m/s
% case3=wind speed=6 m/s
% case4=wind speed=8 m/s
% case5=wind speed=10 m/s
% case6=wind speed=12 m/s
select_case='case6';

switch lower(select_case)
    case 'case1'
        nr=881.7568;      % wtr=8.7  %rpm;
        P=100e3;          %W;
        Io_max=P/Uo
        R_load=Uo/Io_max
        D=0.5304;
        Uin=3962.3;
        fs=1000;
        C=100e-6;
    case 'case2'
        nr=972.973;      % wtr=9.6  %rpm;
        P=225e3;          %W;
        Io_max=P/Uo
        R_load=Uo/Io_max
        D=0.4832;
        Uin=4360.5;
        fs=1000;
        C=100e-6;
    case 'case3'
        nr=1155.4;       % wtr=11.4 %rpm;
        P=350e3;          %W;
        Io_max=P/Uo
        R_load=Uo/Io_max
        D=0.3856;
        %D=0.3056;
        %Uin=5184;
        fs=1000;
        C=100e-6;
    case 'case4'
        nr=1479.7;       % wtr=14.6 %rpm;
        P=800e3;          %W;
        Io_max=P/Uo

```

```

R_load=Uo/Io_max
D=0.2160;
Uin=6615;
fs=1000;
C=100e-6;
case 'case5'
nr=1500;          % wtr=14.8 %rpm;
P=1650e3;        %W;
Io_max=P/Uo
R_load=Uo/Io_max
D=0.2080;
Uin=6682.5;
fs=1000;
C=100e-6;
case 'case6'
nr=1500;          % wtr=14.8 %rpm;
P=2000e3;        %W;
Io_max=P/Uo
R_load=Uo/Io_max
D=0.2;
Uin=6740;
fs=1000;
C=100e-6;
otherwise
disp('Wrong case selection---Case6(Rated values) was selected
by default')
nr=1500;          % wtr=14.8 %rpm;
P=2000e3;        %W;
Io_max=P/Uo
R_load=Uo/Io_max
D=0.2;
Uin=6750;
fs=1000;
C=100e-6;
end

% ng=1500/14.8=101.3514; gearbox ratio
wr=nr*pi/30;
T=(P/wr)
L_boost=10e-3;

% Inductor and capacitor of the Boost with different fs for each case
Ts=1/fs;
% L_boost=((Ts*Uo)/(2*Io_max))*(D*(1-D)^2)
% I_L_ripple=0.3*(Io_max*Uo)/Uin
% L_boost_ideal=Uin*(Uo-Uin)/(Uo*fs*I_L_ripple)
% Uo_ripple=0.1*Uo
% C_min=(Io_max*D)/(fs*0.1*Uo)

sim('PMSG_Rectifier_Ld_Boost')
whos

% Distributing the PMSG-parameters
is_a=PMSG_Output(:,1);
is_b=PMSG_Output(:,2);
is_c=PMSG_Output(:,3);
is_d=PMSG_Output(:,4);
is_q=PMSG_Output(:,5);
vs_d=PMSG_Output(:,6);
vs_q=PMSG_Output(:,7);
hall_a=PMSG_Output(:,8);

```



```

legend('is_d','is_q','Location','NorthOutside','Orientation','horizontal');

%%_PRINT_%%_PRINT_%%_PRINT_%%_PRINT_%%_PRINT_%%_PRINT_%%_PRINT_%%_PRINT
direction=['C:\Dokument\MASTER THESIS\SIMULINK
FILES\PMSG\PMSG+Rectifier+Ld+Boost\figures\'];
name=[direction,'stator currents d-q'];
print('-dpng','-noui','-r300',[name,'.png']);
%%_PRINT_%%_PRINT_%%_PRINT_%%_PRINT_%%_PRINT_%%_PRINT_%%_PRINT_%%_PRINT

% Stator voltages in d-q axes
figure(3);
plot(time,vs_d,'-','LineWidth',2,'MarkerSize',3),grid;
hold on
plot(time,vs_q,':','LineWidth',2,'MarkerSize',3),grid;
hold on
title('stator voltages d-q','fontsi',[16]);
xlabel('time(s)','fontsi',[15]);
ylabel('voltage(V)','fontsi',[15]);
legend('vs_d','vs_q','Location','NorthOutside','Orientation','horizontal');

%%_PRINT_%%_PRINT_%%_PRINT_%%_PRINT_%%_PRINT_%%_PRINT_%%_PRINT_%%_PRINT
direction=['C:\Dokument\MASTER THESIS\SIMULINK
FILES\PMSG\PMSG+Rectifier+Ld+Boost\figures\'];
name=[direction,'stator voltages d-q'];
print('-dpng','-noui','-r300',[name,'.png']);
%%_PRINT_%%_PRINT_%%_PRINT_%%_PRINT_%%_PRINT_%%_PRINT_%%_PRINT_%%_PRINT

% Rotor speed
figure(4);
plot(time,RotorSpeed,'LineWidth',2,'MarkerSize',3),grid;
title('Rotor Speed','fontsi',[16]);
xlabel('time(s)','fontsi',[15]);
ylabel('speed(rad/s)','fontsi',[15]);
legend('Rotorspeed','Location','NorthOutside','Orientation','horizontal');

%%_PRINT_%%_PRINT_%%_PRINT_%%_PRINT_%%_PRINT_%%_PRINT_%%_PRINT_%%_PRINT
direction=['C:\Dokument\MASTER THESIS\SIMULINK
FILES\PMSG\PMSG+Rectifier+Ld+Boost\figures\'];
name=[direction,'Rotor Speed'];
print('-dpng','-noui','-r300',[name,'.png']);
%%_PRINT_%%_PRINT_%%_PRINT_%%_PRINT_%%_PRINT_%%_PRINT_%%_PRINT_%%_PRINT

% Electromagnetic torque
figure(5);
plot(time,Te,'LineWidth',2,'MarkerSize',3),grid;
title('electromagnetic torque','fontsi',[16]);
xlabel('time(s)','fontsi',[15]);
ylabel('torque(Nm)','fontsi',[15]);
legend('Te','Location','NorthOutside','Orientation','horizontal');

%%_PRINT_%%_PRINT_%%_PRINT_%%_PRINT_%%_PRINT_%%_PRINT_%%_PRINT_%%_PRINT
direction=['C:\Dokument\MASTER THESIS\SIMULINK
FILES\PMSG\PMSG+Rectifier+Ld+Boost\figures\'];
name=[direction,'electromagnetic torque'];

```





```

legend('Po','Location','NorthOutside','Orientation','horizontal');

%%_PRINT_%%_PRINT_%%_PRINT_%%_PRINT_%%_PRINT_%%_PRINT_%%_PRINT_%%_PRINT_%%_PRINT
direction=['C:\Dokument\MASTER THESIS\SIMULINK
FILES\PMMSG\PMMSG+Rectifier+Ld+Boost\figures\'];
name=[direction,'Output Power'];
print('-dpng','-noui','-r300',[name,'.png']);
%%_PRINT_%%_PRINT_%%_PRINT_%%_PRINT_%%_PRINT_%%_PRINT_%%_PRINT_%%_PRINT_%%_PRINT

% Rectifier measurements
figure(9);
[AX,H1,H2] = plotyy(time,Isw1,time,Vab),grid;
set(AX(2),'Ylim',[-8000 8000]);
set(AX(2),'YTick',[-8000:1000:8000])
set(AX(1),'Ylim',[-500 500]);
set(AX(1),'YTick',[-500:100:500]);
set(get(AX(1),'Ylabel'),'String','current(A)','fontsi',[15]);
set(get(AX(2),'Ylabel'),'String','voltage(V)','fontsi',[15]);
set(H1,'Line','-','LineWidth',2,'MarkerSize',3);
set(H2,'Line',':','LineWidth',2,'MarkerSize',3);
xlabel('time(s)','fontsi',[15]);
title('Rectifier measurements','fontsi',[16]);
legend('Isw1','Vab','Location','NorthOutside','Orientation','horizontal');

%%_PRINT_%%_PRINT_%%_PRINT_%%_PRINT_%%_PRINT_%%_PRINT_%%_PRINT_%%_PRINT_%%_PRINT
direction=['C:\Dokument\MASTER THESIS\SIMULINK
FILES\PMMSG\PMMSG+Rectifier+Ld+Boost\figures\'];
name=[direction,'Rectifier measurements'];
print('-dpng','-noui','-r300',[name,'.png']);
%%_PRINT_%%_PRINT_%%_PRINT_%%_PRINT_%%_PRINT_%%_PRINT_%%_PRINT_%%_PRINT_%%_PRINT

% Diode measurements
figure(10);
[AX,H1,H2] = plotyy(time,I_Diode,time,V_Diode),grid;
set(get(AX(1),'Ylabel'),'String','current(A)','fontsi',[15]);
set(get(AX(2),'Ylabel'),'String','voltage(V)','fontsi',[15]);
set(H2,'Line','-','LineWidth',2,'MarkerSize',3);
set(H1,'Line',':','LineWidth',2,'MarkerSize',3);
xlabel('time(s)','fontsi',[15]);
title('Diode measurements','fontsi',[16]);
legend('I_diode','V_diode','Location','NorthOutside','Orientation','horizontal');

%%_PRINT_%%_PRINT_%%_PRINT_%%_PRINT_%%_PRINT_%%_PRINT_%%_PRINT_%%_PRINT_%%_PRINT
direction=['C:\Dokument\MASTER THESIS\SIMULINK
FILES\PMMSG\PMMSG+Rectifier+Ld+Boost\figures\'];
name=[direction,'Diode measurements'];
print('-dpng','-noui','-r300',[name,'.png']);
%%_PRINT_%%_PRINT_%%_PRINT_%%_PRINT_%%_PRINT_%%_PRINT_%%_PRINT_%%_PRINT_%%_PRINT

% IGBT measurements
figure(11);
[AX,H1,H2] = plotyy(time,I_IGBT,time,V_IGBT),grid;
set(get(AX(1),'Ylabel'),'String','current(A)','fontsi',[15]);
set(get(AX(2),'Ylabel'),'String','voltage(V)','fontsi',[15]);
set(H2,'Line','-','LineWidth',2,'MarkerSize',3);

```



```

% case6=wind speed=12 m/s
select_case='case4';

switch lower(select_case)
  case 'case1'
    nr=881.7568;      % wtr=8.7  %rpm;
    P=100e3;         %W;
    U=3962.3;
    R=(U^2)/P
  case 'case2'
    nr=972.973;      % wtr=9.6  %rpm;
    P=225e3;         %W;
    U=4360.5;
    R=(U^2)/P
  case 'case3'
    nr=1155.4;       % wtr=11.4 %rpm;
    P=350e3;         %W;
    U=5184;
    R=(U^2)/P
  case 'case4'
    nr=1479.7;       % wtr=14.6 %rpm;
    P=800e3;         %W;
    U=6615;
    R=(U^2)/P
    D=0.2160;
    Id=130;
  case 'case5'
    nr=1500;         % wtr=14.8 %rpm;
    P=1650e3;        %W;
    U=6682.5;
    R=(U^2)/P
    D=0.2080;
    Id=260;
  case 'case6'
    nr=1500;         % wtr=14.8 %rpm;
    P=2000e3;        %W;
    U=6750;
    R=(U^2)/P
    D=0.2;
    Id=310;
  otherwise
    disp('Wrong case selection---Case6(Rated values) was selected
by default')
    nr=1500;         % wtr=14.8 %rpm;
    P=2000e3;        %W;
    U=6750;
    R=(U^2)/P
    D=0.2;
    Id=310;
end

% ng=1500/14.8=101.3514; gearbox ratio
wr=nr*pi/30;
T=(P/wr)

% Losses in the diode rectifier
V_on_diode=3.1;
P_cond_rect=2*2*Id*V_on_diode;
P_cond_rect_percent=P_cond_rect/P*100

% Losses in the IGBT

```

```

V_IGBT=4500;
Von=4;
n_series=1.5*Uo/V_IGBT;
tr=0.78e-6;
tf=6e-6;
K=1.5;
Ps_IGBT=V_IGBT*(tr+tf)*fs/(2*K);
Pc_IGBT=n_series*Von*D*Id;
Ps_IGBT_percent=Ps_IGBT/P*100
Pc_IGBT_percent=Pc_IGBT/P*100

% Losses in the diode
Pc_diode=V_on_diode*(1-D)*Id;
Pc_diode_percent=Pc_diode/P*100

% Losses in the inductor
H=0.14;
Dl=384.7;
ro_L=0.44;
R_L=ro_L*H/(Dl^2);
Pcore=2.2*3741;
Pcopper=R_L*(Id)^2;
Ptot_ind=Pcore+Pcopper;
P_ind_percent=Ptot_ind/P*100

```